

PAPER View Article Online



Cite this: DOI: 10.1039/c7ib00011a

Integrative meta-modeling identifies endocytic vesicles, late endosome and the nucleus as the cellular compartments primarily directing RTK signaling†

Jared C. Weddell and Princess I. Imoukhuede*

Recently, intracellular receptor signaling has been identified as a key component mediating cell responses for various receptor tyrosine kinases (RTKs). However, the extent each endocytic compartment (endocytic vesicle, early endosome, recycling endosome, late endosome, lysosome and nucleus) contributes to receptor signaling has not been quantified. Furthermore, our understanding of endocytosis and receptor signaling is complicated by cell- or receptor-specific endocytosis mechanisms. Therefore, towards understanding the differential endocytic compartment signaling roles, and identifying how to achieve signal transduction control for RTKs, we delineate how endocytosis regulates RTK signaling. We achieve this via a meta-analysis across eight RTKs, integrating computational modeling with experimentally derived cell (compartment volume, trafficking kinetics and pH) and ligand-receptor (ligand/receptor concentration and interaction kinetics) physiology. Our simulations predict the abundance of signaling from eight RTKs, identifying the following hierarchy in RTK signaling: PDGFR β > IGFR1 > EGFR > PDGFR α > VEGFR1 > VEGFR2 > Tie2 > FGFR1. We find that endocytic vesicles are the primary cell signaling compartment; over 43% of total receptor signaling occurs within the endocytic vesicle compartment for these eight RTKs. Mechanistically, we found that high RTK signaling within endocytic vesicles may be attributed to their low volume (5.3 \times 10⁻¹⁹ L) which facilitates an enriched ligand concentration (3.2 μ M per ligand molecule within the endocytic vesicle). Under the analyzed physiological conditions, we identified extracellular ligand concentration as the most sensitive parameter to change; hence the most significant one to modify when regulating absolute compartment signaling. We also found that the late endosome and nucleus compartments are important contributors to receptor signaling, where 26% and 18%, respectively, of average receptor signaling occurs across the eight RTKs. Conversely, we found very low membranebased receptor signaling, exhibiting <1% of the total receptor signaling for these eight RTKs. Moreover, we found that nuclear translocation, mechanistically, requires late endosomal transport; when we blocked receptor trafficking from late endosomes to the nucleus we found a 57% reduction in nuclear translocation. In summary, our research has elucidated the significance of endocytic vesicles, late endosomes and the nucleus in RTK signal propagation.

Received 13th January 2017, Accepted 11th April 2017

DOI: 10.1039/c7ib00011a

rsc.li/integrative-biology

Insight, innovation, integration

We find that receptor signaling primarily stems from endocytic vesicles, late endosomes and the nucleus, whereas membrane signaling is relatively low for every RTK tested. We determine a physiological ranking of RTK signaling: PDGFRβ has the highest and FGFR1 has the lowest absolute membrane signaling among the RTKs analyzed. We identify that high receptor activation within endocytic vesicles is due to their low volume, facilitating ligand enrichment and leading to sustained receptor phosphorylation. We observe significant nuclear signaling for all RTKs, which requires a late endosome pathway. We find that extracellular ligand concentrations regulate absolute compartment signaling; increasing the extracellular ligand concentration increases nuclear signaling.

Department of Bioengineering, University of Illinois at Urbana-Champaign, 1304 W Springfield Ave., 3233 Digital Computer Laboratory, Urbana, IL 61801, USA. E-mail: pii@illinois.edu

† Electronic supplementary information (ESI) available. See DOI: 10.1039/c7ib00011a

Introduction

Understanding and controlling signal transduction could lead to new therapeutic approaches for many pathologies, including

cancers^{1,2} and vascular diseases.^{3,4} Typically, membrane receptors are the prime targets for controlling signal transduction, as they are the initial elicitors of cell responses from extracellular signal transduction (e.g., ligands).^{5,6} Accordingly, signal transduction pathways have been established for many membrane receptors. 7-10 However, signal transduction involves the integration of extracellular cues with intracellular processes, such as receptor endocytosis, phosphorylation events, and second messengers. 11,12 As such, membrane-bound receptors alone do not define this integrative signaling occurring within a cell. Our understanding of these intracellular signaling events is complicated, as endocytosis is affected by cell and receptor type. 13,14 Therefore, to achieve signal transduction control for any receptor, a delineation between the physical principles and cell- or receptor-specific physiology mediating endocytosis is needed. Such an analysis would serve as a "signaling template," providing signaling fundamentals that could be applied to examine cell- or receptor-specific signaling dynamics 14,15 and directing experimental research to treat pathological conditions. Computational systems biology, the integration of mathematical modeling and experimental biological data, 16 is well poised to provide this analysis.

Previous computational systems biology studies have identified that significant receptor signaling occurs intracellularly (e.g., via internalized receptors). ^{17,18} This is an important advancement from the early view that endocytosis only functioned to terminate membrane receptor signaling,¹⁷ a view derived from key findings that while both ligand-bound and unbound receptors are trafficked to lysosomes, ligand-bound receptors internalize \sim 10-fold faster. ¹⁹⁻²¹ However, computational models uncovered a different story: cells exhibiting prolonged receptor signaling and enhanced cell responses exhibit less receptor recycling, leading to intracellular ligand-receptor accumulation. 22,23 Later experimental studies validated these computational predictions; Di Guglielmo et al. identified active endosomal epidermal growth factor receptor (EGFR), along with phosphorylated endosomal-Shc, Grb2 and mSOS signaling molecules.²⁴ Thus, computational models have helped to offer new interpretations into receptor signaling. As such, a computationally-based signaling template that examines intracellular-based signaling across several RTKs could further enhance knowledge of intracellular signaling mechanisms.

Knowledge of intracellular receptor signaling is primarily based upon studies of EGFR, which is often researched due to its important role in pathologies, including cancers. 8,25,26 Intracellular signaling analyses should be extended to other receptors; particularly those with high intracellular localization, such as vascular endothelial growth factor receptor-1 (VEGFR1), where $\sim 80\%$ is localized intracellularly. ^{27–29} Indeed, intracellular VEGFR1 has been empirically identified as critical to the VEGFR1 signaling axis; an intracellular VEGFR1 isoform, expressing the phosphotransferase domain and the carboxy terminal tail, activates the Src kinase, increasing breast cancer cell invasiveness.³⁰ Likewise, studies of intracellular fibroblast growth factor receptor-1 (FGFR1) show that it increases KRTAP5-6 gene expression, a known migration promoter, and decreases GRINA gene expression, a known migration

inhibitor.³¹ Therefore, extending intracellular-based signaling analyses to receptors outside the EGFR family is a necessary step toward building a signaling template.

Here, we engineered such a signaling template, by integrating computational modeling with experimental receptor data, and meta-analyzing signaling through eight tyrosine kinases receptors (RTKs): EGFR, FGFR1, Insulin-like growth factor 1 receptor (IGFR1), platelet-derived growth factor receptors alpha (PDGFRα) and beta (PDGFRβ), VEGFR1, VEGFR2, and Tie2. We quantified receptor phosphorylation, a post-translational modification, associated with each endocytic compartment, to weigh the signaling contribution from each intracellular compartment. The eight RTKs we examine all exhibit the same key signaling mechanisms post ligand stimulation: (1) carboxy-terminal phosphorylation, (2) adapter protein binding to these phosphorylated carboxy-terminal sites, and subsequent (3) adapter protein phosphorylation and recruitment and activation of second messenger proteins to propagate intracellular signaling. We model RTK phosphorylation, since it is the key signaling mechanism facilitating the second messenger signaling that ultimately directs cell responses such as survival, proliferation, and migration. 32-34 For example, cell proliferation results from phosphorylation of the VEGFR2 Tyr¹¹⁷⁵ site, whereas phosphorylation at the VEGFR2 Tyr¹²¹⁴ site is linked to cell migration.³² Furthermore, the concentration of receptor phosphorylation has been shown to quantitatively correlate with cell response; 35,36 EGFR phosphorylation levels are proportional to amount of cell migration.³⁶

Overall, this study predicts the importance of endocytic vesicles, late endosomes and the nucleus in RTK signaling and offers new mechanistic insights into RTK nuclear translocation. This study also provides a physiologically relevant signaling template, which can be applied to direct experiments to measure or control cell and/or receptor-specific signaling.

Results

The computational signaling template or "meta-model" for RTK signaling (Fig. 1) includes compartment volumes (Table 1), pH (Table 1), and trafficking kinetics (Table 2), which are held the same for these eight RTKs, but ligand-receptor concentrations and interaction kinetics are RTK specific (Table 3).37-45 We identify trafficking kinetics by fitting to experimental endocytosis data (Fig. S1, ESI†) that quantified receptor localization on the plasma membrane (Fig. S1A, ESI†), through the nucleus (Fig. S1B, ESI†), including the intermediate endosome (Fig. S1C and D, ESI†), and lysosome (Fig. S1E and F, ESI†). With this data, we simulate RTK signaling as the integrated receptor phosphorylation over time, 46,47 described as the "integrated signaling". NOTE: the term integrated signaling and other such terms are defined in Table 4. The integrated signaling of an RTK is analyzed in each compartment and normalized to the membrane integrated signaling in Table 3.

The extent of membrane signaling is dependent on the RTK

We find that after four hours, the total phosphorylated receptor is highly variable across the eight RTKs with Integrative Biology Paper

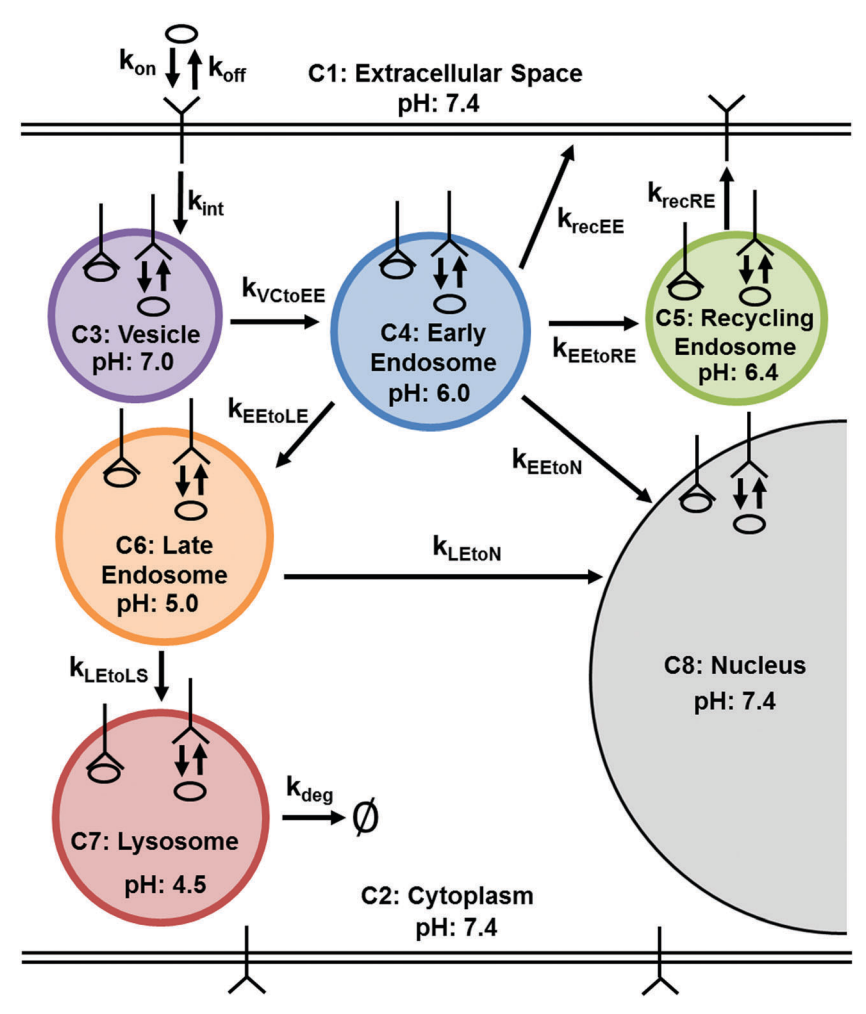


Fig. 1 RTK endocytosis signaling template. Ligand–receptor interactions and trafficking occur across seven compartments (C1–C8), defined by their volume, pH, and ligand–receptor kinetics (Table 1). In each compartment, a free receptor can bind a free ligand to form a ligand–receptor complex, as shown. Rate parameters describing the transitions between intracellular compartments are also given. Abbreviations and descriptions of trafficking are as follows: on = ligand binding, off = ligand unbinding, int = receptor internalization, VC = vesicle, EE = early endosome, recEE = recycling early endosome, recRE = recycling endosome, LE = late endosome, N = nucleus, LS = lysosome, and deg = degradation.

Table 1 Model compartment parameters. Compartments are defined by their spherical diameter, volume, pH, and ligand–receptor kinetics as shown. All compartments are assumed spherical except for the extracellular space. Note that k_{off} rates of the ligands dissociation from receptors are regulated by pH, as described by eqn (4) (Materials and methods)

Compartment	Spherical diameter	Volume (cm ³)	pН	$k_{\rm on} ({\rm molecules}^{-1} {\rm s}^{-1})$	$k_{\rm off} ({ m s}^{-1})$
Extracellular space	<u>—</u> ,	2.5×10^{-6}	7.4	6.6×10^{-9}	1.0×10^{-3}
Cytoplasm	18 μm ²¹²	1.6×10^{-9}	7.4	_	_
Endocytic vesicle	100 nm ^{154,155}	5.2×10^{-16}	7.0	$3.2 imes 10^{1}$	1.5×10^{-3}
Early endosome	1 μm ¹⁵⁷	5.2×10^{-13}	6.0	$3.2 imes 10^{-2}$	3.8×10^{-3}
Recycling endosome	100 nm ^{154,155}	5.2×10^{-16}	6.4	$3.2 imes 10^{-2}$	2.6×10^{-3}
Late endosome	2 μm ¹⁵⁷	4.2×10^{-12}	5.0	4.0×10^{-3}	1.0×10^{-2}
Lysosome	2 μm ¹⁵⁷	4.2×10^{-12}	4.5	0	$1.0 imes 10^2$
Nucleus	14 μm ²¹³	1.4×10^{-9}	7.4	1.2×10^{-5}	1.0×10^{-3}

PDGFR β having the highest integrated signaling on the membrane. Indeed, the plasma membrane PDGFR β signaling is 3.1 \times 10³-fold greater than FGFR1, which has the lowest absolute membrane signaling (Table 3). By analyzing the three RTK-specific parameters – receptor concentration [R], ligand concentration [L] and ligand–receptor dissociation

constant $K_{\rm d}$ – one observes that differential RTK signaling is determined by the complex concentration, which is defined as $\frac{[R][L]}{\nu}$. Indeed, FGFR1 has the lowest complex concentration

 $\overline{K_d}$. Indeed, FGFR1 has the lowest complex concentration among the eight RTKs probed, attributed primarily to its low serum concentration of ligand. Conversely, PDGFR β has the

Table 2 Model implemented trafficking kinetics compared to previous endocytosis models. Trafficking parameters for movement between each endocytic compartment. Different rates were fit for phosphorylated (pR) and unphosphorylated (R) receptors. Rates are represented as mean \pm standard deviation, as determined by parameter fitting. Kinetic parameters used in several previous endocytosis models are given as a comparison. Dashes indicate rates that were not used in previous models. All rates are given in units of s⁻¹. Abbreviations are defined in the footnotes

Parameter	Implemented rate	VEGFR2 ¹⁶⁰	EGFR ³⁷	EGFR ²¹⁰	HER2 ²¹¹
k _{int} (R)	$1.5 \times 10^{-3} \pm 1.6 \times 10^{-4}$	1.6×10^{-3}	5.0×10^{-5}	0	1.7×10^{-4}
$k_{\rm int}$ (pR)	$1.0\times 10^{-2}\pm 2.3\times 10^{-3}$	1.7×10^{-2}	5.0×10^{-5}	3.5×10^{-3}	7.2×10^{-4}
$k_{\text{deg}}\left(\mathbf{R}\right)$	$1.0 imes 10^{-4} \pm 1.0 imes 10^{-5}$	3.8×10^{-4}	6.7×10^{-4}	1.3×10^{-4}	7.0×10^{-5}
k_{deg} (pR)	$1.0\times 10^{-4}\pm 1.0\times 10^{-5}$	9.6×10^{-2}	6.7×10^{-4}	3.3×10^{-4}	7.0×10^{-5}
k_{recEE} (R)	$3.2\times 10^{-4}\pm 1.6\times 10^{-4}$	7.8×10^{-2}	5.0×10^{-3}	5.3×10^{-4}	1.1×10^{-3}
k_{recEE} (pR)	$3.2\times 10^{-4}\pm 1.6\times 10^{-4}$	9.4×10^{-2}	0	3.3×10^{-4}	1.1×10^{-3}
k_{recRE} (R)	$8.6\times 10^{-3}\pm 1.8\times 10^{-3}$	_	_	_	
k_{recRE} (pR)	$8.6 imes 10^{-3} \pm 1.8 imes 10^{-3}$	_	_	_	_
$k_{\text{VCtoEE}}\left(\mathbf{R}\right)$	$7.7 \times 10^{-6} \pm 4.3 \times 10^{-6}$	_	_	_	_
k_{VCtoEE} (pR)	$3.7 \times 10^{-4} \pm 4.2 \times 10^{-5}$	_	_	_	_
k_{EEtoRE} (R)	$8.1 imes 10^{-5} \pm 1.5 imes 10^{-5}$	_	_	_	_
k_{EEtoRE} (pR)	$8.1 imes 10^{-5} \pm 1.5 imes 10^{-5}$	_	_	_	_
$k_{ m EEtoLE}$ (R)	$1.8 \times 10^{-3} \pm 3.0 \times 10^{-4}$	_	_	_	_
k_{EEtoLE} (pR)	$4.5 \times 10^{-3} \pm 9.0 \times 10^{-4}$	_	_	_	_
k_{EEtoN} (R)	$5.0 \times 10^{-4} \pm 8.3 \times 10^{-5}$	_	_	_	_
$k_{\rm EEtoN}$ (pR)	$5.0 \times 10^{-4} \pm 8.3 \times 10^{-5}$	_	_	_	_
$k_{\text{LEtoLS}}\left(\mathbf{R}\right)$	$7.5 \times 10^{-5} \pm 9.1 \times 10^{-6}$	_	_	_	_
$k_{ m LEtoLS}$ (pR)	$6.7 \times 10^{-4} \pm 5.9 \times 10^{-5}$	_	_	_	_
k_{LEtoN} (R)	$3.3 \times 10^{-4} \pm 1.3 \times 10^{-5}$	_	_	_	_
$k_{ m LEtoN}$ (pR)	$3.3 \times 10^{-4} \pm 8.3 \times 10^{-5}$		_	_	_

Int: internalization. Deg: degradation. recX: recycling of receptors from compartment X to the cell membrane. X to Y: RTK trafficking from compartment X to compartment Y. EE: early endosome. RE: recycling endosome. VC: endocytic vesicle. LE: late endosome. N: nucleus. LS: lysosome.

Table 3 Integrated signaling within each endocytic compartment for various RTKs. Mean integrated signaling in each compartment, relative to the membrane, in addition to interaction kinetics and receptor concentrations on the given cell type, for the eight studied RTKs. Receptor concentrations are all taken from human cells in healthy pathology. A brief description of each cell type is given in the footnotes. Interaction kinetics are given for pH = 7.4. Ligand concentrations are taken from serum concentrations. The total membrane integrated signaling over 4 hours after ligand stimulation is given for each RTK. Table is ranked and shaded by total membrane signaling: lighter red indicates lower absolute receptor signaling, darker red indicates higher absolute receptor signaling

		FGF2-	Ang2-	VEGFA-	PDGFBB-	VEGFA-	IGF1-	EGF-	PDGFAA-
		FGFR1	Tie2	VEGFR1	PDGFRα	VEGFR2	IGFR1	EGFR	PDGFRβ
	Receptors/cell	$2.8 \cdot 10^{4}$ 39	$1.8 \cdot 10^{3}$ 38	$9.9 \cdot 10^{2}$ 38	$5.1 \cdot 10^{3}$ 38	$1.9 \cdot 10^{3}$ 38	$2.5 \cdot 10^{4}$ 40	$1.1 \cdot 10^{5}$ 214	$5.3 \cdot 10^{438}$
SIS	Cell Type	COS7	HUVEC ^a	HUVEC ^a	HDF ^b	HUVEC ^a	NIH-3T3	MCF-10A	HDF ^b
iete	$k_{on}(M^{-1}s^{-1})$	9.6.104 43	$6.0 \cdot 10^{3}$ 45	$3.0 \cdot 10^{7}$ 126	$7.8 \cdot 10^6$ 215	$1.0 \cdot 10^{7}$ 126	$2.7 \cdot 10^{5}$ 44	$3.0 \cdot 10^{7}$ 37	$8.8 \cdot 10^{3}$ ²¹⁵
Parameters	$k_{\rm off}(s^{-1})$	5.9·10 ⁻³ 43	6.1.10-4 45	1.0.10-3 126	7.6.10-3 215	$1.0 \cdot 10^{-3}$ 126	1.2.10-3 44	3.8·10 ⁻³ 37	1.5.10-4 215
Pa	Ligand in Serum	2.2 216	1865 217	160 216	8506 ²¹⁸	160 ²¹⁶	1.65·10 ⁵	917 220	1769 ²²¹
	(pg/mL)								
50	Membrane	1.0	1.0	1.0	1.0	1.0	1.0	1.0	1.0
Integrated signaling relative to membrane	Endocytic Vesicle	386	90	75	73	80	75	58	57
gna to ne	Early Endosome	10	9.2	8.0	2.4	8.4	2.7	2.9	8.9
rated signarelative to membrane	Recycling	9.8·10 ⁻²	8.8·10 ⁻²	7.6·10 ⁻²	1.9·10 ⁻²	$8.0 \cdot 10^{-2}$	2.3·10 ⁻²	2.6·10 ⁻²	8.7·10 ⁻²
ted lati	Endosome								
gra re me	Late Endosome	108	54	52	23	55	27	27	41
nte	Lysosome	3.2·10 ⁻⁴	1.6.10-4	1.6·10-4	6.8·10 ⁻⁵	1.6·10 ⁻⁴	8.1·10 ⁻⁵	8.1.10-5	1.2.10-4
T I	Nucleus	17	9	37	35	33	38	33	16
	Total membrane								
	integrated	1.5·10 ¹	$8.9 \cdot 10^2$	$1.7 \cdot 10^3$	$2.3 \cdot 10^3$	$3.1 \cdot 10^3$	$1.1 \cdot 10^4$	$3.4 \cdot 10^4$	$4.7 \cdot 10^4$
	signaling								
	(p-Receptor·time)								
shrana rignating. Low Hig									
hrane signaling: LOW - Ingl									

Membrane signaling:

^a Human umbilical vein endothelial cells. ^b Human dermal fibroblast.

greatest complex concentration; hence the greatest integrated signaling, which is attributed to both the high serum concentration of its ligand and high receptor concentration (Table 3).

Given these physiological conditions modeled, we predict a hierarchy in membrane signaling, as follows: PDGFR β > IGFR1 > EGFR > PDGFR α > VEGFR1 > VEGFR2 > Tie2 > FGFR1.

This journal is @ The Royal Society of Chemistry 2017

Table 4 Terminology list. List of terms used within the manuscript, their definition, and how they are computed if they are a mathematical term. Note that the definitions given are provided in the context of this manuscript, i.e. how each term is defined within this manuscript

Term	Definition	Computation
Response	The physiological process of receptors producing a global cell	_
Receptor signaling OR	response through phosphorylation, and subsequent second messenger activation The dynamic activation of a receptor following ligand stimulation	pR
signaling Integrated signaling	The total receptor phosphorylation over time	$\int_{0}^{t} \mathbf{P} \mathbf{R}_{Cn} dt$ From time $t = 0$ to $t = t$ For compartment n (Fig. 1)
Compartmentalized signaling	The receptor signaling stemming from a single endocytic compartment	pR_{Cn} For compartment n (Fig. 1)
Membrane-based receptor signaling OR	The receptor signaling stemming from the cell membrane specifically (compartment 1, Fig. 1)	pR_{C1}
Membrane signaling Intracellular-based receptor signaling	Receptor signaling stemming from all intracellular compartments (compartments 2-7, Fig. 1)	$\sum_{n=2}^{7} pR_{Cn}$
Nuclear signaling	Receptor signaling stemming from the nucleus (compartment 7, Fig. 1)	pR_{C7}
Nuclear translocation Complex concentration	Receptor trafficking from the cell membrane to the nucleus The amount of bound ligand and receptors	$\frac{-}{[R][L]} \frac{K_d}{K_d}$
		where K_d is the ligand–receptor dissociation constant

RTK signaling primarily occurs intracellularly

While the hierarchy in RTK signaling (phosphorylated receptor) on the plasma membrane offers insight into receptor sensitivity, our model reveals a hierarchy in compartment signaling. We observe that following four hour stimulation, signaling occurs primarily on endocytic vesicles > late endosome > nucleus ~ early endosome > membrane> recycling endosome > lysosome. Indeed, 43% of total phosphorylated receptor resides on endocytic vesicles versus <1% of total receptor signaling occurring on plasma membrane (Table 3). The significance of the nucleus in signaling is also important to note, where it is predicted to comprise anywhere between 3.3% of total phosphorylated FGFR to 27% of total phosphorylated EGFR within a cell (Table 3). Altogether, these simulations show that receptor signaling primarily occurs in intracellular compartments.

Compartmentalization leads to two primary receptor signaling trends

The hierarchy in RTKs and in compartments that we observe is based on integration over four hours; however signaling is dynamic so examining the full signaling time-course, early and late, offers greatest insight on how signaling changes. To visualize RTK signaling dynamics, we chose one ligand-receptor pair of focus: Ang2-Tie2. The Ang2-Tie2 system offers new insight into signaling, as it has not been previously modeled. Moreover, an examination of Table 3 shows that each of the RTKs preserve the compartmental hierarchy, so examining one ligand-RTK system offers insights into the trends of the other RTKs. Compartmentalized signaling for the seven other RTKs is also given in the ESI† (Fig. S2-S8). Towards the goal of visualizing RTK signaling dynamics we specifically examine the duration of receptor signaling, a parameter that directs differential cell responses⁴⁸ in each compartment. We find that receptors associated with the membrane (Fig. 2A), endocytic vesicle (Fig. 2B), early endosome (Fig. 2C), and recycling endosome (Fig. 2D) have similar signaling with activation and decay constants of \sim 68 minutes. Another set of compartments with similar signaling profiles are the late endosome (Fig. 2E) and lysosome (Fig. 2F); here we observed that receptors have a 49 minute activation constant and 144 minute decay constant. The nuclear compartment does not follow either receptor signaling trend (Fig. 2G), instead exhibiting the slowest receptor signaling, containing \sim 3% of the total phosphorylated Tie2 at four hours after ligand stimulation. Overall, the signaling profile of the Ang2-Tie2 system allows us to rank the compartmental signaling trends as rapid (membrane, endocytic vesicle, early endosome and recycling endosome), slow (late endosome and lysosome), and identifying the slowest compartment as the nucleus.

Phosphorylated receptors primarily associate with endocytic vesicles and late endosomes

Since compartmentalization affects the time-constants for receptor signaling, we should expect the distribution of receptor signaling to change at early and late time-points. To identify which compartments dominate signaling over time, we continue our representative receptor, Tie2, examining its compartmentalized signaling (Fig. 2H). As receptor trafficking conventions would dictate, we observe that endocytic vesicles serve as an early locale of receptors and late endosomes serve as a latter receptor compartment. More specifically, five minutes after ligand stimulus, ~22% of the total phosphorylated receptors reside within endocytic vesicles, whereas <1% are associated with all other compartments (Fig. 2H). Conversely, three hours

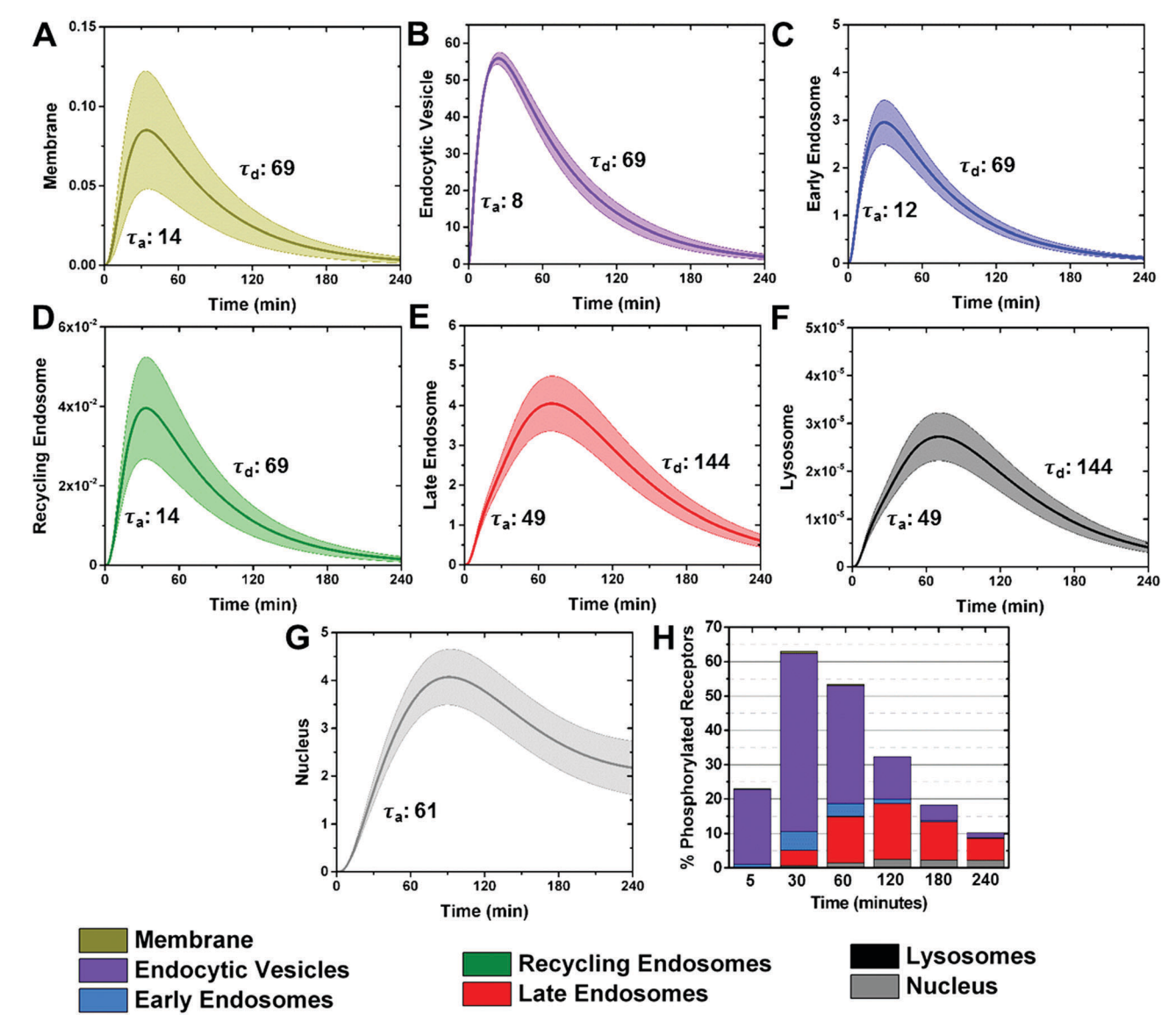


Fig. 2 RTK signaling compartmentalization, represented by Tie2 signaling, primarily occurs within endocytic vesicles early, and late endosomes late, after ligand stimulus. The percent of phosphorylated Tie2 relative to total cell receptors are given on (A) the cell membrane, (B) endocytic vesicles, (C) early endosomes, (D) recycling endosomes, (E) late endosomes, (F) lysosomes, and (G) in the nucleus. Tie2 signaling is used as a representative for all eight RTKs; signaling compartmentalization for the other seven RTKs is provided in the ESI† (Fig. S2-S8). The activation time constant (τ_a , time from ligand stimulus to 63.2% max signaling) and decay time constant (r_d, time from max signaling to 36.8% max signaling) in minutes are also given for each compartment. Data is represented as mean \pm standard deviation from 10 000 Monte Carlo simulations, randomly seeded across the possible trafficking kinetics (Table 2). (H) Mean phosphorylated receptor localization relative to total cell receptors at 5, 60, 120, 180 and 240 minutes after ligand stimulus.

after ligand stimulus, $\sim 11\%$ of the total phosphorylated receptors are within late endosomes, whereas <5% are associated with all other compartments (Fig. 2H). It is important to note the staggered importance of the early endosome and nuclear compartments in signaling.

Small size and sustained signaling facilitates high endocytic vesicle signaling

Since endocytic vesicles both offer the highest integrated signaling (Table 3) and comprise a bulk of phosphorylated receptor at early times (Fig. 2), we explain why the endocytic vesicle emerges as a significant compartment to signaling.

We hypothesize that the small endocytic vesicle volume (Table 1) offers an enriched ligand environment that favors receptor ligation. To test this hypothesis, we compare receptor signaling within a single endocytic vesicle to receptor signaling at the membrane, where ligands are not highly concentrated (Fig. 3A). We block receptor trafficking to and from the single endocytic vesicle and membrane to ensure receptor signaling only depends on the individual compartment. Furthermore, we assume one ligand for one receptor; for Tie2, which has 1800 membrane receptors (Table 3),38 this equates to 1800 (84 pg mL⁻¹ or 1.2 pM) Ang2 molecules, which is within the range of previously measured serum ligand concentrations (Table 3).

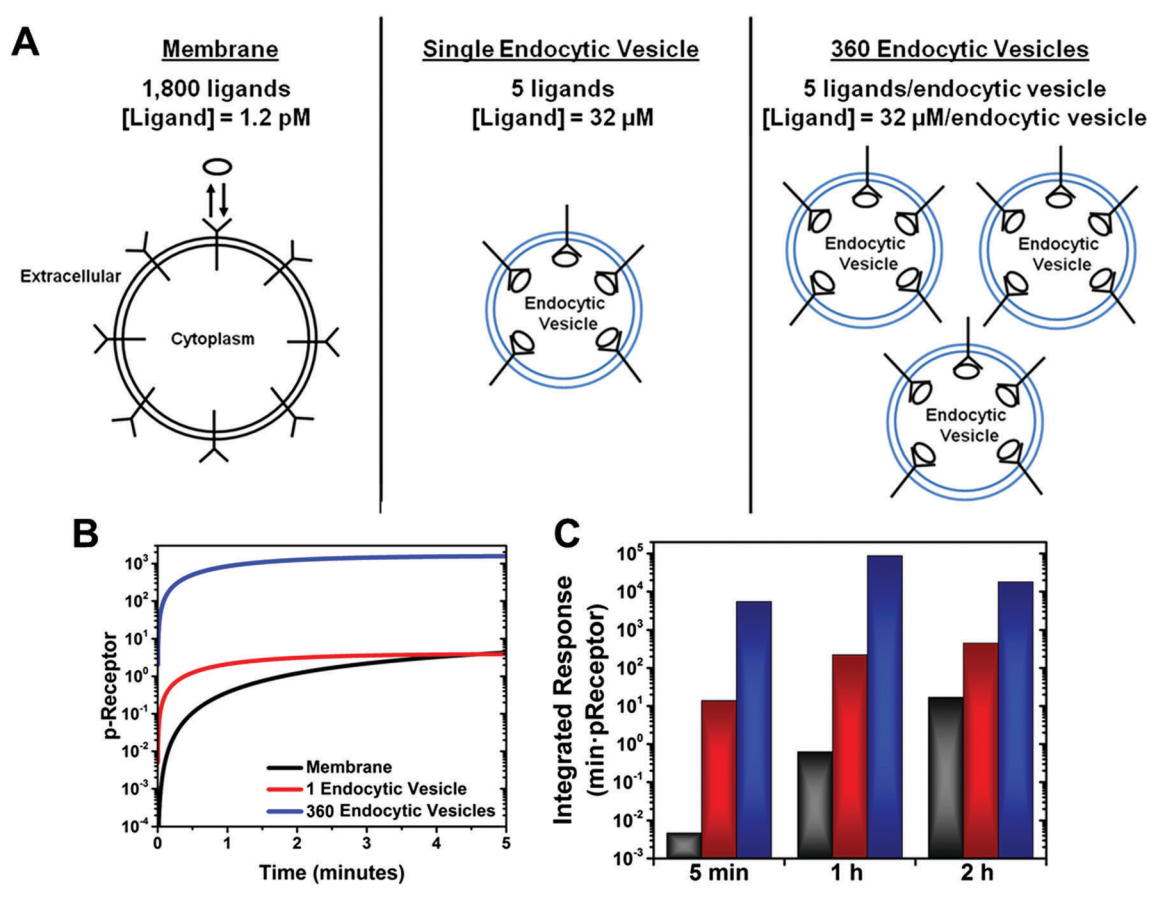


Fig. 3 Receptor clustering within endocytic vesicles facilitates high, sustained receptor signaling. (A) Schematic showing the three simulations cases. (B) Receptor signaling versus time was simulated on the cell membrane, on a single endocytic vesicle, or when all receptors were contained on endocytic vesicles. (C) The integrated signaling at 5 minutes, 1 hour and 2 hours are given for each case.

We assume 5 receptors associate with a single endocytic vesicle, an assumption based on previous experimental observations of receptor concentrations of vesicles. 49-51 Together, this would give 5 ligand molecules (1.1 mg mL⁻¹ or 16 µM) in a single endocytic vesicle. With these concentrations, we find that <1%of the membrane receptors are phosphorylated at 60 minutes after ligand stimulation (Fig. 3B). Conversely, we find that $\sim 80\%$ of the endocytic vesicle receptors are phosphorylated at equilibrium, which is reached within 5 minutes after ligand stimulation (Fig. 3C). We also examine the case where all 1800 receptors are associated with endocytic vesicles, yielding 5 receptors per endocytic vesicle for 360 endocytic vesicles total. We find that ~1500 receptors are phosphorylated across the 360 endocytic vesicles at equilibrium (Fig. 3C). Thus, we show that the low compartment volume of the endocytic vesicle can sustain and amplify receptor signaling.

Endocytic compartment signaling can be tuned by the extracellular ligand concentration

Having established that the endocytic vesicle relevance is related to its small volume, we examine whether simulation parameters can be tuned to increase or decrease endocytic vesicle signaling. Continuing with the Ang2-Tie2 as a representative axis, we alter ligand and receptor concentrations and

ligand-receptor binding kinetics and observe where compartmentalized signaling occurs (Fig. 4). NOTE: compartmentalized signaling for the other seven RTKs is given in the ESI† (Fig. S9-S15). We notice that k_{off} and k_{on} have inverse effects on receptor signaling: increasing ligand–receptor dissociation (k_{off}) decreases RTK signaling in all compartments with the exception of the endocytic vesicles (Fig. 4A). Whereas, increasing ligand-receptor association (k_{on}) appears to facilitate receptor trafficking by increasing signaling to both the late endosome and nucleus, while decreasing signaling in the endocytic vesicles (Fig. 4B).

Since ligand-receptor interactions kinetics cannot be easily altered therapeutically, we also compare the ability for ligand versus receptor concentration to regulate RTK signaling. Increasing either ligand (Fig. 4C) or receptor concentrations (Fig. 4D) leads to a similar effect as increasing ligation kinetics: increased trafficking away from endocytic vesicles to the other compartments: some increased endosomal localization and significant increases in nuclear translocation. Moreover, changes in ligand concentration direct receptor signaling to a greater extent than changes in receptor concentration: increasing ligand decreases endocytic vesicle signaling up to 47%, relative to normal Ang2 levels (Table 3 and Fig. 4C). However, we only observe a 23% decrease in Tie2 signaling when receptor concentrations vary over the same range, or 6 orders of

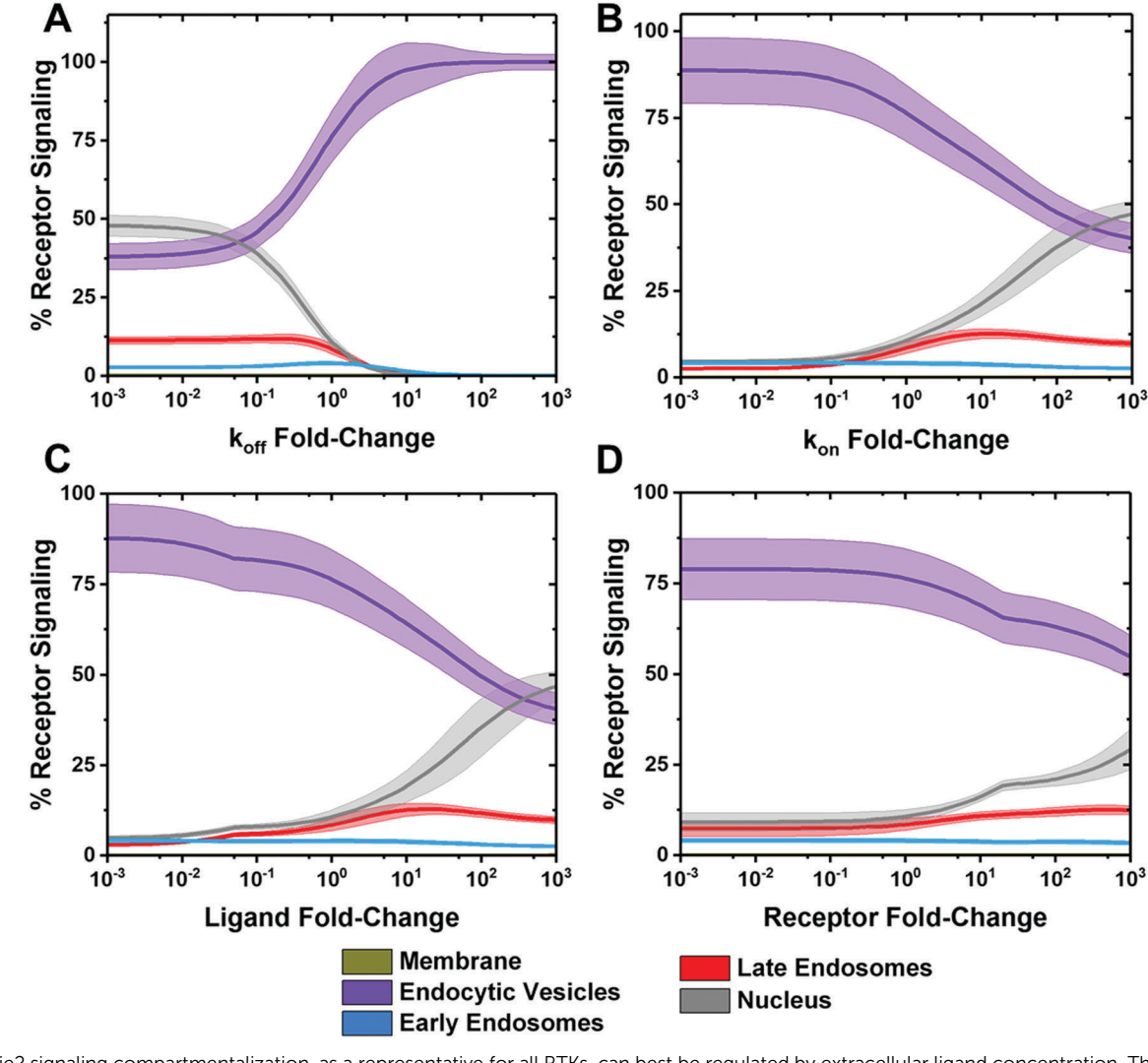


Fig. 4 Tie2 signaling compartmentalization, as a representative for all RTKs, can best be regulated by extracellular ligand concentration. The percent of total receptor signaling associated with each compartment were quantified with altered Ang2-Tie2 parameters, provided as representative for all RTKs. The compartmentalized signaling for the other seven RTKs studied here can be found in the ESI† (Fig. S9-S15). Recycling endosome- and lysosome-based receptor signaling are not included as they account for <0.01% total receptor signaling. The four parameters changed are (A) ligand-receptor off-rate, (B) ligand-receptor on-rate, (C) ligand concentration, and (D) receptor concentration. Data is represented as mean \pm standard deviation from 10 000 Monte Carlo simulations, randomly seeded across the possible trafficking kinetics (Table 2)

magnitude (Fig. 4D). These results show that under physiological ranges of ligand and receptor concentrations, endocytic vesicle signaling can be best regulated by changing extracellular ligand concentration. Additionally, the primary compartments affected by changes in ligand, receptor, or affinity are the endocytic vesicles and the nucleus.

Membrane receptor translocation to the nucleus primarily occurs through a late endosome pathway

In addition to endocytic vesicles, our compartment hierarchy (Table 3) and signaling dynamics simulation (Fig. 2H) show that late endosomes and nucleus are important compartments for signaling. To better understand how trafficking affects signaling, we simulate test cases where individual endocytic pathways are blocked and observe how nuclear signaling is

affected for our representative RTK: Tie2 (Fig. 5). We predict that minimal nuclear translocation occurs when late endosomalto-nuclear trafficking is blocked; under that condition, we observe a 57% reduction in nuclear translocation (Fig. 5). Whereas, maximal nuclear translocation occurs when early endosomal-to-late endosomal trafficking is blocked; here we observed a 270% increase in nuclear accumulation of the representative receptor, phosphorylated Tie2. Late endosomalto-lysosomal trafficking inhibition also results in a significant increase in nuclear translocation of phosphorylated Tie2 (140% increase). Conversely, blocking the other pathways (receptor recycling, early endosomal-to-nucleus and early endosomal-tolate endosomal) is not as effective in shifting the distribution phosphorylated receptor in nucleus. Therefore, while nuclear translocation requires transport through early endosomes, we

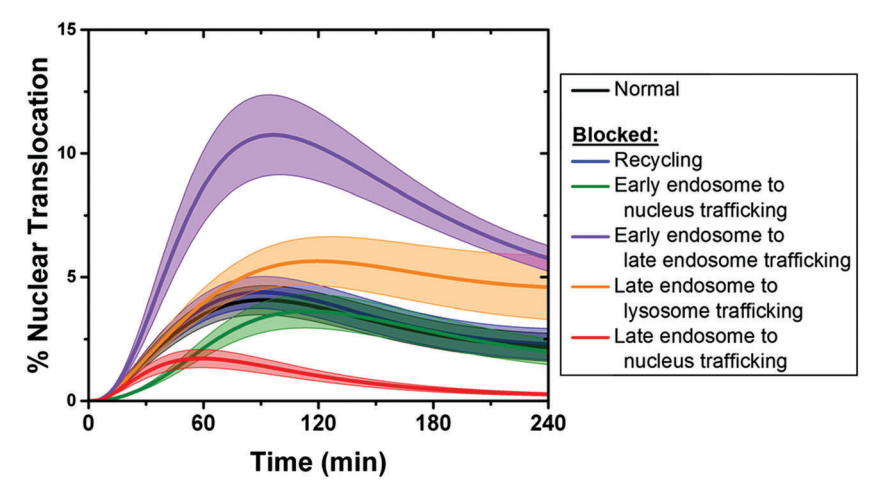


Fig. 5 Tie2 nuclear translocation, as representative for all RTKs, is effectively inhibited by blocking late endosome trafficking. Percent total Tie2 translocated to the nucleus, as representative for all RTKs, when endocytic pathways are blocked, and cells are ligand stimulated for 4 hours. Inhibited pathways involve receptor movement from the early endosomes and late endosomes (Fig. 1). These pathways are the recycling pathways (blue), trafficking from early endosomes to the nucleus (green), trafficking from early endosomes to late endosomes (purple), trafficking from late endosomes to lysosomes (orange), and trafficking from late endosomes to the nucleus (red). Data is represented as mean \pm standard deviation from 10 000 Monte Carlo simulations, randomly seeded across the possible trafficking kinetics (Table 2)

predict that inhibiting late endosomal-to-nuclear trafficking would be most efficient at preventing RTK nuclear translocation.

Nuclear-based signaling for any RTK is determined by the extracellular ligand concentration

Since our sensitivity analysis reveals that the intracellular signaling of Tie2 can be tuned by the extracellular Ang2 concentration (Fig. 4), we return to our meta-model to examine whether extracellular ligand concentration, affinity, or the complex concentration can predict compartmentalized receptor signaling for any of the eight RTKs. To this end, we perform a correlation analysis, assuming a lognormal fit, between mean nuclear signaling and the RTK parameters for these eight RTKs (Fig. 6). We continue our focus on the nuclear compartment, given our predictions on its importance to signaling. Signaling for the other compartments is included in the ESI† (Fig. S16-S19) with the exception of the recycling endosomes and lysosomes. They are excluded, because they account for <0.01% total receptor signaling across all eight RTKs. We find that nuclear signaling has a low correlation with the receptor concentration (Fig. 6A, $R^2 = 0.08$) and the ligand-receptor dissociation constant, or affinity (Fig. 6B, $R^2 = 0.17$), implying that these parameters have low weight in determining the hierarchy in RTK nuclear signaling. We observe that extracellular ligand concentration does a better job of characterizing nuclear signaling (Fig. 6C, $R^2 = 0.47$), indicating that it carries the highest weight among the three parameters (receptor concentration, affinity, and ligand concentration); indeed, this correlation analysis predicts that increasing the extracellular ligand concentration one order of magnitude will increase nuclear signaling 3.2-fold. Furthermore, the complex concentration, which is comprised of the three parameters, provides the best overall predictor of RTK nuclear signaling (Fig. 6D, $R^2 = 0.75$), confirming that nuclear signaling is mediated by these three RTK parameters. The low weight of both receptor concentration and ligand-receptor dissociation and high weight of extracellular ligand concentration to RTK nuclear also holds for the other endocytic compartments (Fig. S16-S19, ESI†). Overall, this meta-analysis between RTK parameters and receptor signaling indicates that the extracellular ligand concentration is the RTK parameter that best regulates receptor signaling.

Discussion

Our integrative RTK meta-modeling approach is the first time that these eight RTKs, all of which are critical to disease (e.g., cancer, 1,2,52,53 cardiovascular disease, 3,4 stroke 54,55) have been comparatively modeled. This meta-modeling led us to four important findings. First, receptor signaling primarily stems from endocytic vesicles, late endosomes and the nucleus (3-27%), whereas membrane signaling is relatively low for every RTK tested. Second, we determine a physiological ranking of RTK signaling: PDGFRβ has the highest and FGFR1 has the lowest absolute membrane signaling. Third, high receptor activation within endocytic vesicles is due to their low volume, facilitating ligand enrichment and leading to sustained receptor signaling. Finally, we find that the extracellular ligand concentration regulates absolute compartment signaling; increasing the extracellular ligand concentration one order of magnitude increases nuclear signaling 3.2-fold. Together these results have implications for accurately quantifying receptor signaling, optimizing therapeutics targeting RTK pathways, understanding drug resistance to such therapeutics, and genetic regulation mediated by RTK signaling, which we describe below.

Integrative computational modeling and biological data allows novel insights into RTK signaling

The four important findings presented in this study are derived from our meta-modeling approach that integrates computational



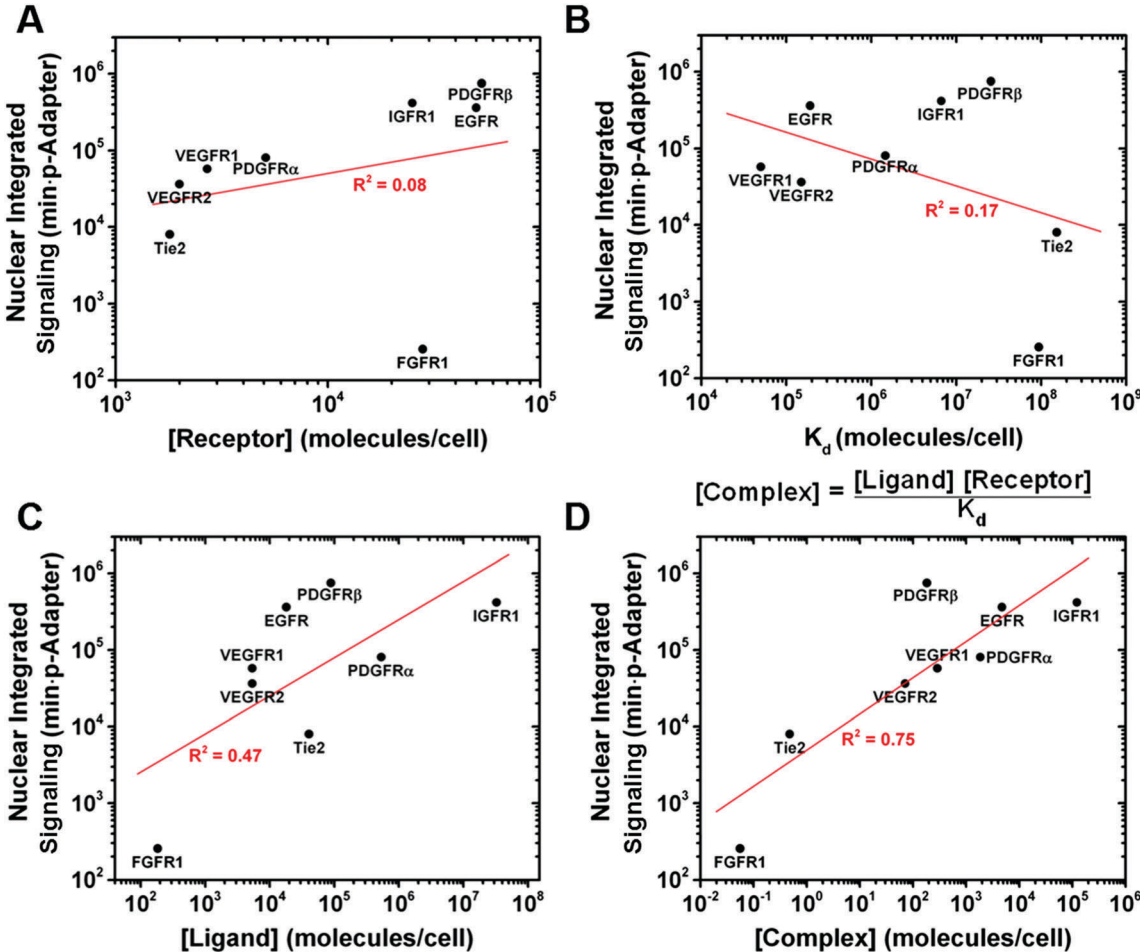


Fig. 6 Nuclear signaling is determined by extracellular ligand concentration. Nuclear signaling among the eight RTKs was fit to the following RTK parameters: (A) receptor concentration, (B) extracellular ligand concentration, (C) ligand-receptor dissociation constant, and (D) complex concentration, defined as the product of extracellular ligand concentration and membrane receptor concentration divided by the ligand-receptor dissociation constant. The R² goodness of fit, using a lognormal fit assumption, is given for each RTK parameter. Correlation analyses between RTK parameter and RTK signaling are also given for the membrane (Fig. S16, ESI†), endocytic vesicle (Fig. S17, ESI†), early endosome (Fig. S18, ESI†), and late endosome (Fig. S19, ESI†) compartments; recycling endosome and lysosome signaling are not included as they account for < 0.01% total receptor signaling.

modeling with physiological data. It is important to note that while these conclusions are predicted and not experimentally derived, they could only be found through computational investigation. Indeed, experimentally defining receptor signaling across each endocytic compartment requires capturing receptor colocalization with a biomarker specific to an endocytic compartment, such as EEA1 for early endosomes. 56,57 However, these experimental techniques are limited: they generally provide qualitative data, making accurate quantitation of receptor localization difficult.58-62 Furthermore, due to the dynamic nature of endocytic compartment transitions, which involves fusion of endocytic vesicles to create early endosomes, these biomarkers can have cross reactivity with multiple endocytic compartments. 60,61,63 Likewise, biomarker expression within a single endocytic compartment varies dynamically, further complicating quantitative colocalization measurements. 64 Therefore, accurately quantifying receptor signaling within specific endocytic compartments is a difficult feat to accomplish experimentally. Furthermore, experimental measurements are specific to the cell and receptor type

examined by nature, and results obtained for a single receptor may not be applicable to all RTKs. This highlights one of the primary advantages of our computational meta-modeling approach: the ability to delineate the complex mechanisms specific to cell or receptor types and generalize how endocytosis directs RTK signaling. Furthermore, our integrative modeling technique can be applied to direct experimental research examining cell- or receptor-specific signaling, optimizing experiments and reducing investigation time and costs.

Experimental support for compartment dynamics: implications for drug delivery

Our analysis of signal duration show two primary signaling compartmentalization patterns: (1) rapid receptor signaling, which we observe in the membrane, endocytic vesicles, early endosomes and recycling endosomes and (2) slow receptor signaling, which we observed in late endosomes and lysosomes. Prior experimental studies offer support to our predicted signaling dynamics. 17,65-67 For example following ligand stimulation,

PDGFRs⁶⁷ and VEGFR2⁶⁸ are primarily phosphorylated within endosomal compartments early (30 minutes), then shift to downstream endocytic compartments late (2 hours). However, these experimental studies do not differentiate receptor signaling at different endocytic compartments, which is the fundamental advancement of our model. This temporal receptor signaling pattern highlighted by our model is particularly useful for optimizing time-dependent drug delivery. 69-71 Specifically, our simulations suggest that drug regimens targeting endocytic vesicle signaling would need to be initiated within 60 minutes following ligand stimulus to be effective. After this time, receptors will predominantly reside in late endosomes, which would render endocytic drugs ineffective. Thus, our results that receptor signaling occurs in distinct early and late trends agree with experimentally observed receptor signaling trends, and provides a tool for optimizing dynamic drug delivery.

Importance of targeting RTKs, intracellularly: VEGFRs and tumor angiogenesis

Our result that RTK signaling primarily occurs intracellularly both provides insight into optimizing drug treatments and can be applied to targeting those RTKs that are primarily localized intracellularly. For example, VEGFR2 is often targeted to inhibit tumor angiogenesis, 72,73 and $\sim 50\%$ of total VEGFR2 is localized within endosomes. 74,75 Our result that VEGFR2 is highly phosphorylated within endosomes relative to the cell membrane implies that inhibiting membrane VEGFR2 may not effectively prevent VEGFR2 signaling; instead, intracellular VEGFR2 needs to be targeted. Indeed, experimental studies have shown that RTK inhibitors that penetrate the plasma membrane are more effective at reducing receptor signaling.76,77 Additionally, Wicki et. al. show that loading a VEGFR2-targeting antibody into liposomes facilitating cell uptake of the antibody and results in a 77% greater decrease in tumor volume over exposing to VEGFR2 antibody alone in a HT-29 colon cancer mouse model.⁷⁸ Thus, inhibiting membrane RTKs alone may not be sufficient to prevent signaling, and our model further underlies the importance of intracellular-based RTK targeting.

Experimental support for endocytic vesicle importance

Our finding of the signaling concentration occurring in the low volume endocytic vesicle can also serve as a model for the receptor clustering occurring within membrane lipid rafts.^{79,80} Indeed, receptor clustering has been optogenetically manipulated to induce signaling through PDGFRs and other receptors.81 Moreover, our finding that signaling primarily occurs within endocytic vesicles suggests that endocytic vesicles should be the primary target to modulate RTK signaling. Experimental observations appear to validate these findings for all eight RTKs tested wherein ERK phosphorylation is decreased by inhibiting the endocytosis of EGFR, 82 FGFR1, 83 IGFR1, 84 PDGFRβ85 and VEGFR2.86 Similarly, inhibiting recycling, which would facilitate PDGFRα accumulation in endocytic vesicles, is found to increase ERK phosphorylation.87 Therefore, our results and piro experimental data indicate that targeting the residence of RTKs in

endocytic vesicle receptors or receptor clusters is an ideal approach to tune receptor signaling.

Importance of targeting RTKs, intracellularly: EGFRs and cancer cell drug resistance

Our result that RTK signaling primarily occurs within endocytic vesicles can shed additional light on cancer drug resistance. Drugs that only target membrane receptors and do not affect endocytic vesicle receptors would be sub-optimal given our finding that membrane signaling accounts for merely 1% of the total cell signaling. Indeed, the literature offers an example of such failed-targeting in gefitinib, a small molecule inhibitor that blocks the EGFR ATP binding site. It is used to treat nonsmall cell lung cancer (NSCLC). Gefitinib is effective only in cell types where it inhibits intracellular-based EGFR signaling, such as in NSCLC PC9 cells; gefitinib inhibits EGFR endocytosis, but not EGFR signaling at the cell membrane. 88,89 Conversely, QG56 cells have aberrant endocytosis, natively, so this cell type has been found to be gefitinib-resistant.88 Thus, our simulations offer guidance in RTK inhibition, suggesting improved efficacy when inhibiting intracellular receptor signaling, while offering insights into the mechanisms leading to reduced drug efficacy.

Experimental support for nuclear translocation

We predicted that all membrane RTKs undergo significant nuclear translocation, representing between 3.3% and 27% total receptor signaling, following ligand stimulation. Furthermore, we find that nuclear translocation can be tuned by extracellular ligand concentration or late endosomal targeting. Nuclear translocation is a process that occurs for many RTKs. 90-92 Indeed, all eight RTKs examined in this study have been qualitatively observed within the nucleus, except PDGFRβ, which lacks experimental investigation (reviewed in; 93 specifically - Tie2; 94,95 EGFR; 96-98 FGFR1; 99-101 | IGFR1; 102-105 | PDGFRa; 106,107 | VEGFR1; 108,109 VEGFR2¹¹⁰⁻¹¹⁴). It is important to note that nuclear translocation can involve retrograde transport of receptor fragments from endosome to endoplasmic reticulum and Golgi apparatus to nucleus. 115-117 However, our model does not focus on fragments.

Importance of targeting nuclear translocation: implications for gene expression

While the full implications of nuclear translocation have not been fully delineated, it is known that nuclear translocated RTKs can directly interact with proteins to regulate gene expression and elicit global cell responses. 92,93,118,119 In one study, Wang et al. shows that membrane ERBB2 undergoes nuclear translocation to directly bind the COX-2 promoter and stimulate its transcription in cancer cells, thus increasing the anti-apoptotic, proangiogenic and metastatic potential of cancer cells. 120 Receptors undergoing nuclear translocation can also indirectly regulate gene expression by shuttling adapter proteins to the nucleus; ERBB4 binds and transports the adapter STAT5 to the nucleus, initiating gene expression. 121 Therefore, our model findings on the importance of ligand and endosomal trafficking in nuclear translocation suggests that

one can increase gene expression by either increasing the extracellular ligand concentration or blocking early endosomal to late endosomal trafficking. Conversely, gene expression may be decreased by preventing endocytosis to late endosomes (*e.g.*, Rab 7 inhibition).

Computational recommendation: cell-receptor-specific trafficking rates

This computational model is designed as a signaling template: a generalized model that can be extended to account for specific cell or RTK machinery. As such, these quantitative results are dependent on our assumption that all RTKs, and all cell types, have the same trafficking kinetics. However, different cell types, such as cancerous cells compared to healthy cells, may have different trafficking rates, which would alter the model predictions. In this case, the distribution of receptors in compartments would shift. Therefore, extending our model to specific RTKs and cell lines, and updating the model with cell/receptor-specific trafficking data would offer the greatest accuracy to the specific system.

Computational recommendation: late endosomal modeling

An additional model extension would be further examining the importance of the late endosome, since we find that a significant portion of RTK signaling stems from this compartment. An, important, sub-compartment, specific to late endosomes are the intraluminal vesicles, called multivariate bodies (MVB). RTK signaling does occur in MVBs,²⁷ but the proteins involved in MVB trafficking vary depending on the RTK or cell type. For instance, RTK association with Cbl is considered mandatory for intraluminal vesicle formation; 14,122 however, various non-small cell lung cancer cells (NSCLC) express EGFR mutants that do not associate with Cbl. 123 This indicates that these NSCLCs either do not form intraluminal vesicles, or they use different cellular machinery, natively. 123 While our model does not account for MVBs, further modeling could include this complexity, particularly towards identifying late-endosomal specific approaches for targeting RTK signaling.

Deriving new experimental insight from models

Our model exemplifies the power of computation to predict system behavior based on the properties of the system. 124 Computational models can also help identify critical parameters of the system: parameters that when changed can have greater effect on system behavior, an well-established area of computational research. 125 A recent example of gleaning important system properties comes from a pharmacokinetic model of an anti-angiogenic drug in tumor. Here, sensitivity analysis of the key receptors mediating vascularization: VEGFRs and neuropilin, revealed that a range of 2000-6000 VEGFRs and ~80 000 neuropilins on tumor cells could change VEGF concentrations in tumor by over 3-fold.⁴² Most anti-angiogenic agents aim to decrease vascularization by either inhibiting VEGF or its receptors, so the fact that VEGFRs can so significantly affect VEGF concentrations suggests that models should have accurate concentrations of these receptors. Indeed, such

model analysis has opened the door to receptor quantification as a critical step in computational model development. ^{126–131} New experimental studies quantifying VEGFR, PDGFR, and Tie2 receptors ^{75,132–134} have led to new insight into challenges in treating ischemic disease, ¹³² characterization of tumor heterogeneity, ^{126,134} and suggest the possibility of ligand signaling across-families. ³⁸ These studies on receptor quantification demonstrate that models, including the one presented here, can guide optimal experimental design.

Experimental recommendation: manipulating compartmental hierarchy

Our model reveals that RTK signaling compartmentalization is hierarchical, as follows: endocytic vesicles > late endosome > nucleus ~ early endosome > membrane > recycling endosome > lysosome, with similar hierarchy in the sensitivity of these compartments to change (Fig. 2). These findings are based on the general assumption that trafficking rates vary between 1-2 orders of magnitude from known trafficking rates. Therefore, experimental studies having the greatest potential to advance our understanding of endocytosis signaling would manipulate trafficking rates, particularly those of the endocytic vesicles to significantly increase or decrease RTK signaling. This can be done by targeting membrane-to-vesicle plasmamembrane trafficking machinery e.g., SNARE proteins, lipid rafts, caveolin, etc.; many of which have been delineated and manipulated. 135,136 Inhibiting or blocking membrane-to-vesicle trafficking proteins would increase membrane residence -(e.g., dynasore inhibition of dynamin);¹³⁷ thereby decreasing the endocytic signaling contribution and likely decreasing overall RTK signaling since the signal amplification of the small-volume vesicle would be lost. Whereas, overexpressing these membraneto vesicle trafficking proteins or treating with drugs that promote endocytosis should lead to significant increases in RTK signaling. For example, phorbol esters promote endocytosis, 138,139 and the BHK-21 cell stimulation with phorbol esters increases the number of endocytic vesicles up to 2-fold, and even normalizes endocytosis in cells with Rab mutations. 140 Another option to increase RTK signaling would be to treat cells with neomycin to prevent endocytic vesicle fusion into early endosomes, thereby retaining receptors within endocytic vesicles. 141,142 Alternatively, our results show that late endosomes are required for nuclear translocation; to this end, the Rab GTPases are an ideal protein target. 143-146 For example, Rab7 regulates early to late endosome trafficking; mutating Rab7 prevents VEGFR2 endocytosis to late endosomes, causing VEGFR2 accumulation in early endosomes. 143 Thus, our results indicate that treating cells with dynasore to prevent endocytosis, with phorbol esters or neomycin to increase endocytic vesicle signaling, or targeting Rab proteins to decrease nuclear translocation, are high-potential experimental targets to tune RTK signaling.

Experimental recommendation: manipulating RTK signaling hierarchy

Our meta-modeling finding that extracellular ligand concentration significantly regulates RTK signaling offers computational

support to the common biology practice of ligand treatment. Indeed, ligand-treatment enables studies of cell behavior and even activation of cell differentiation. 147-149 Building upon the importance of ligand is the importance of the complex, where we find the following hierarchy in signaling abundance on the membrane: PDGFR β > IGFR > EGFR > PDGFR α > VEGFR1 > VEGFR2 > Tie2 > FGFR1 (Fig. 6D). Since many of these receptors activate similar second messengers, including MAPK, Akt, and others, 150-153 our computational template offers opportunities to manipulate intracellular signaling on cells carrying different combinations of these receptors. For example if a researcher aims to increase migratory behavior in a cell carrying IGFR1 and FGFR1, our model suggests that manipulating IGFR1 would provide greater effect, provided the cell has similar properties as those modeled. To make a cell-specific determination of which receptor to target, an experimentalist would

simply examine the complex formation $\left(\frac{[\mathbf{R}][\mathbf{L}]}{K_{\mathrm{d}}}\right)$.

Conclusion

Our comparative examination of eight commonly studied RTKs offers insight into their compartmentalized signaling. Overall, this study predicts that receptor signaling can best be controlled by targeting intracellular-based receptors, particularly endocytic vesicles, to regulate receptor signaling or late endosomes to regulate nuclear translocation. Future studies can adapt the signaling template presented here to direct the regulation of specific receptor signaling in pathological cases.

Materials and methods

Model assumptions

The following are the primary model assumptions, with brief justification. Additional discussion and justification for each assumption are additionally provided in the following Materials and methods sections.

First, we make the following assumptions regarding compartment geometry: (1) we assume all compartments, except for the extracellular space, are spherical, and are not RTK specific. We list the spherical diameters in Table 1. This assumption is based on studies showing average compartment sizes that do not vary by more than 60% for cells expressing our RTKs. 154,155 (2) We assume that recycling endosomes are the same size as endocytic vesicles. This assumption is based on data showing that recycling endosomes and endocytic vesicles have similar sizes. 154,156 (3) We assume that lysosomes are the same size as late endosomes. This is justified as late endosome and lysosome markers both appear on similar sized compartments. 157 Finally, with regards to our compartment size assumptions, we show that increasing or decreasing compartment size by 10-fold causes a negligible (<1% for non-nuclear compartments) change in RTK signaling, via sensitivity analysis (Fig. 7).

Second, we make the following assumptions regarding kinetics: (1) we assume that all RTKs have trafficking kinetics that are within the ranges of known RTK dynamics. We list the known and unknown trafficking rates in Table 2. (2) We obtain trafficking kinetics by fitting to experimental data, as described in the Materials and methods (Fig. S1, ESI†). (3) We assume that the receptor phosphorylation and dephosphorylation rates are the same for all eight RTKs and remain the same across all model compartments. This is a typical model assumption shown to retain model physiological accuracy. 37,158-162 (4) While dimerization is an important process that is known to contribute to RTK signaling, 163-166 we do not model this as a separate step, instead, we assume all receptors are present in a pre-dimerized, inactive state, activated by ligand binding. This model assumption of pre-dimerized receptors is an established model assumption that allows accurate receptor signaling quantifications, 42,126 and is based on evidence that VEGFR2 pre-dimerization may stabilize a ligand-dimeric complex. 166,167 (5) We assume that the ligand-receptor dissociation constant changes with compartment pH (Table 1), based on empirical measurements directly measuring ligand-receptor dissociation constant versus pH. 37,168 Furthermore, we determine that increasing or decreasing the pH within any compartment by 0.5 exerts a negligible effect on RTK signaling (<2% for non-nuclear compartments), via sensitivity analysis (Fig. 8). (6) We assume all cell receptors are initially localized to the cell membrane and all ligands are initially localized extracellularly (Table 3). This is a typical model initialization scheme. 19,169,170 It physiologically correlates with experiments where membrane receptors are labeled with a biomarker that is tracked, following ligand stimulation. 171,172 (7) We do not assume that RTK concentrations are the same across the cells, so we literature mine these data from quantitative studies across multiple cell lines (Table 3). This assumption is based on known variations in RTK concentrations on the plasma membrane. 38,128 This is also based on prior computational model sensitivity analyses showing that receptor densities can significantly affect model predictions.42

Computational modeling to predict RTK signaling within endocytosis in a generalized manner

The purpose of this study is to understand how cell physiology (volume, pH, trafficking) directs compartmentalized receptor signaling fundamentally. As such, incorporating receptorspecific trafficking or post-endocytic fates is outside the scope of our study; thus, we use the same cell physiology for each RTK, and examine RTK parameters independent of cell physiology. To delineate the physical principles governing endocytosis from cell- and receptor-specific physiology, we create a computational model that generalizes endocytosis across multiple cell-types and RTKs. Specifically, trafficking kinetics are generalized by incorporating biological data obtained from multiple cell lines, while receptor concentrations are cell-specific. However, it is important that the parameters implemented are consistent within a single RTK. For example, the IGFR1 ligand-receptor interaction kinetics hold for all cell lines. 40 This methodology to aggregate, or assume,

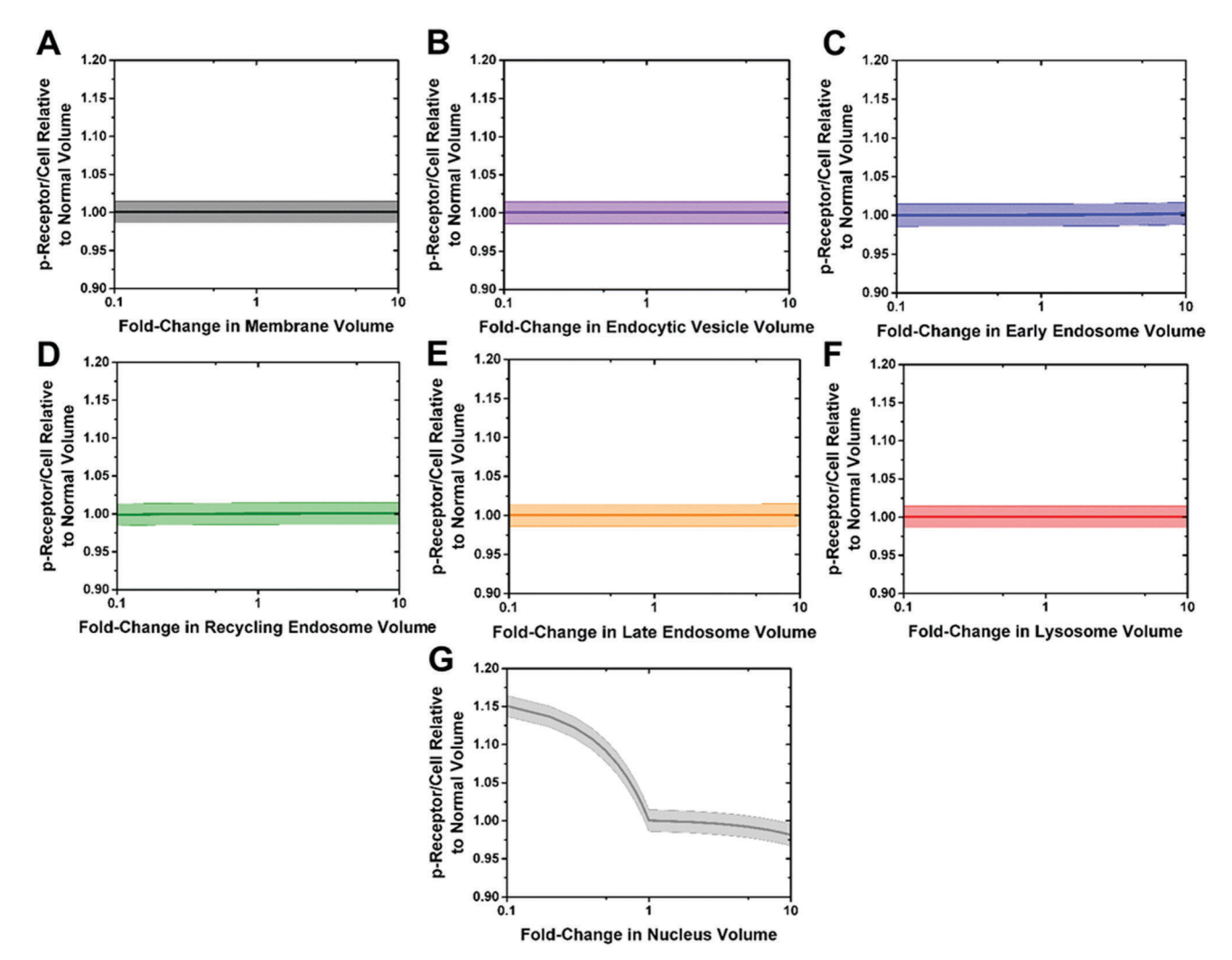


Fig. 7 Compartment volume only affects nuclear signaling. RTK signaling within each compartment is quantified while altering compartment volume 0.1- to 10-fold the physiological value (Table 1). Data is represented as mean \pm standard deviation from 10 000 Monte Carlo simulations, randomly seeded across the possible trafficking kinetics (Table 2)

biological data from multiple sources retains the ability for computational models to provide new insight into a biological system, albeit at a generalized manner. 173 As our goal is to understand RTK signaling within endocytosis generally, we implement this methodology to integrate data across multiple biological sources. Likewise, to allow for generalized investigation into endocytosis, we do not account for endocytosis mechanisms and machinery that differs by cell-type, such as membrane curvature, 174 fluidity, 175 or internalization mechanism (i.e. clathrin- or caveolin-mediated endocytosis). 176 Furthermore, we do not account for how cell machinery differs within an individual cell, such as how membrane composition differs at the plasma membrane compared to early endosomes, 177 which may facilitate receptor dephosphorylation and transient signaling. 178 Additionally, we use receptor phosphorylation as our terminal model output, as signaling molecule activation has localization constraints outside the scope of this study; for example, activation of the signaling molecules PI3K^{179,180} is constrained to the membrane.

Model compartmentalization

The model contains eight compartments representing standard receptor endocytosis (Fig. 1) as follows: 11,181-183 (i) ligandreceptor binding on the plasma membrane; (ii) receptor internalization, including ligands and other receptor- and membrane-bound proteins via endocytic vesicles; (iii) endocytic vesicle fusion into early endosomes; (iv) recycling from early endosomes back to the cell membrane; (v) endosomal maturation into late endosomes; (vi) late endosomal protein trafficking to lysosomes for degradation; (vii) early endosomes and lysosomes trafficking receptors to the nucleus. We assume all compartments, except for the extracellular space, are spherical (Table 1). We assume that recycling endosomes are the same size as endocytic vesicles, as they bud off the early endosomes. Furthermore, we assume that lysosomes are the same size as late endosomes. The extracellular space volume is 0.5 cm³, shared equally between 2×10^5 cells, based on typical conditions used in 24-well plates. 184 To control for compartments Integrative Biology Paper

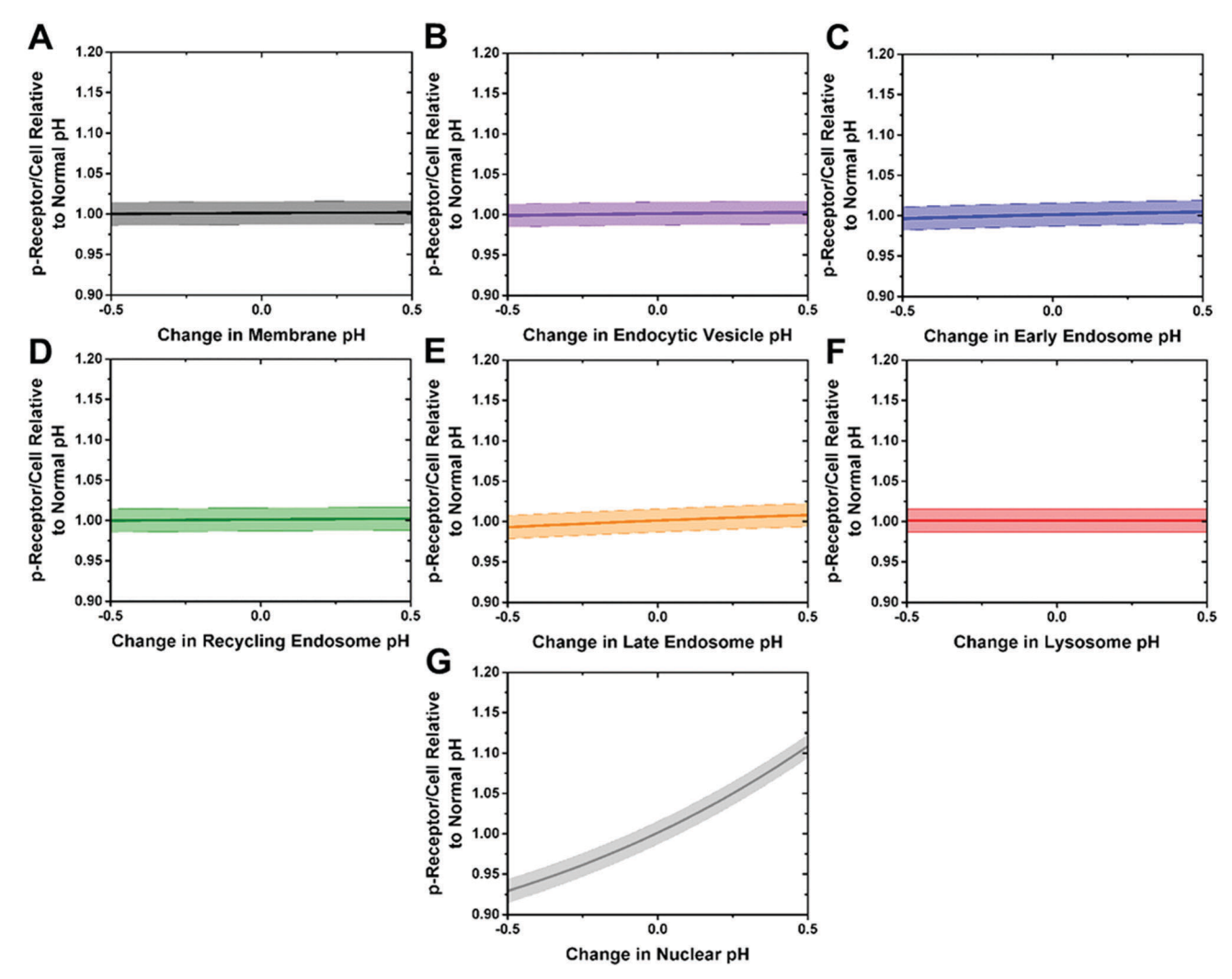


Fig. 8 Compartment pH only affects nuclear signaling. RTK signaling within each compartment is quantified while altering compartment pH 0.5 less and 0.5 more the physiological value (Table 1). Data is represented as mean \pm standard deviation from 10 000 Monte Carlo simulations, randomly seeded across the possible trafficking kinetics (Table 2).

being contained within the cytoplasm volume, we assume the available cytoplasmic volume for protein interactions is one tenth the total volume (Table 1). To ensure our volume assumptions do not alter RTK signaling, we conduct sensitivity analyses altering each compartment volume, individually, across a physiological range and quantify RTK signaling within that compartment (Fig. 7). We find that, other than the nucleus, volume of each compartment does not significantly alter RTK signaling within that compartment (Fig. 7). Thus, our volume assumptions do not significantly alter compartmentalized RTK signaling.

Ligand-receptor interactions

In all model compartments (Fig. 1), we employ a generalized ligand-receptor interaction model using the following chemical reactions:

$$L + R \underset{k_{\text{off}_{1}, \mathbf{P}}}{\overset{k_{\text{on}_{L-R}}}{\Longleftrightarrow}} L: \mathbf{R}$$
 (1)

$$L:R \underset{k_{dp}}{\overset{k_p}{\longleftrightarrow}} L:pR \tag{2}$$

$$L:pR \xrightarrow{k_{\text{off}_{L-R}}} L + R \tag{3}$$

where L is the ligand, R is the unphosphorylated receptor, pR is the phosphorylated receptor, colons indicate bound proteins, $k_{\text{on}_{\text{L-R}}}$ is the ligand-receptor on-rate, $k_{\text{off}_{\text{L-R}}}$ is the ligandreceptor off-rate, k_p is the receptor phosphorylation rate $(1 \times 10^{-2} \text{ s}^{-1160})$, and k_{dp} is the receptor dephosphorylation rate (1 \times 10⁻³ s⁻¹ 160). We also provide a complete list of model reactions in the Supplementary materials and methods (ESI†). Note that the receptor phosphorylation and dephosphorylation rates are the same for all eight RTKs and remain the same across all model compartments. Using generalized phosphorylation and dephosphorylation rates is a typical model assumption, 37,158-162 while retaining model physiological accuracy. For example, our implemented phosphorylation and dephosphorylation rates were taken from a study by Tan *et al.*, which accurately predicted VEGFR2 and ERK phosphorylation dynamics. ¹⁶⁰ These rates also agree well with phosphorylation rates measured for multiple proteins and phosphorylation sites. ^{185,186} Furthermore, each compartment has additional trafficking or degradation reactions (Table 2). Our model assumes all receptors are present in a pre-dimerized, inactive state. We assume that ligand binding activates the pre-dimerized receptors and results in receptor phosphorylation and signaling, a process shown to occur physiologically across multiple RTKs. ^{163–166} Furthermore, dimerization mechanisms are RTK dependent; thus, we do not incorporate dimerization in our meta-model to ensure that receptor phos-

phorylation is dependent only on cell physiology and localization.

Ligand-receptor kinetics

Paper

As ligands and receptors are trafficked throughout the cell the dissociation constant between them changes based on the pH of the compartment in which they reside (Table 1). Similar pH-mediated ligand-receptor kinetics have been constructed for EGF-EGFR interactions in early endosomes. 37,168 Our pH-based kinetic alteration is derived from these studies, but expands upon them to account for more endocytic compartments. First, we determined typical pH for each compartment based on experimental measurements. 11,187,188 Next, we identified how pH mediates ligand-receptor interactions. 168,189-194 For example, the Lauffenburger lab showed that the ligandreceptor dissociation constant increases with decreasing pH for all growth factors they examined. 191 Also, this phenomena that protein binding weakens at lower pH occurs for many protein types, and is not specific to ligand-receptor interactions. 195,196 Previous research has found that ligand-receptor interactions are strongest at pH 7.4, the typical pH of the extracellular space, cytoplasm and nucleus, 197 but weaken as the pH is decreased. 189 For instance, ligand-receptor dissociation constants increase 2- to 3-fold as pH decreases from 7.4 to 6.0189,190 which corresponds with the typical pH of early endosomes. 11 At pH 5.0 in late endosomes, 11 dissociation constants increase ~10-fold. 190 Ligand-receptor interactions no longer occur below pH 5.0, such as in lysosomes.11 We fit the ligand-receptor off-rate as an exponential function to these average pH values by

$$k_{\text{off}} = 1.21 \cdot e^{-0.96 \text{pH}}$$
 (4)

where pH < 5.0 has an infinite off-rate allowing no ligand-receptor interactions (Table 1). It should be noted that different ligand–receptor off-rates are affected by pH changes to different extents; 191,193 the Lauffenburger lab found that the dissociation rate for TGF-alpha increases ~ 60 -fold at pH 6.0 relative to pH 7.4, whereas the EGF dissociation rate increases ~ 30 -fold. 191 However, as all growth factors were observed to undergo increased ligand–receptor dissociation constants with decreased pH, 191 we use this exponential relationship for all eight RTKs, to again remove receptor-specific considerations and provide generalized results. To ensure our pH assumption does not alter RTK signaling, we conduct sensitivity analyses altering each compartment pH, individually, across a physiological range and quantify RTK signaling within that compartment (Fig. 8).

We find that, other than the nucleus, compartment pH does not significantly alter RTK signaling within that compartment (Fig. 8). Thus, our pH assumption does not significantly alter compartmentalized RTK signaling.

Defining ligand and receptor concentrations

We initialized the model such that all cell receptors were initially localized to the cell membrane and all ligands were localized extracellularly (Table 3), a typical model initialization scheme. 19,169,170 Physiologically, this would be a case where membrane receptors are labeled with a biomarker before growth factor simulation occurs. Thus, receptors that are synthesized and inserted into the membrane would not be quantified, as no biomarker is available to label them. Similarly, receptors that are contained intracellularly initially and are recycled to the membrane would also not be labeled; therefore, we do not account for any receptors initially contained intracellularly. Our model therefore tracks and quantifies only receptors that are localized to the plasma membrane prior to ligand stimulation. All receptor and ligand concentrations are implemented as molecules/cell, where concentration conversions from mass/volume to moles/volume were done as necessary using the following ligand molecular weights - Ang2: 70 kDa, 198 EGF: 74 kDa, ¹⁹⁹ FGF-2: 18 kDa, ²⁰⁰ IGF-1: 7.6 kDa, ²⁰¹ PDGF-AA: 30 kDa, ²⁰² PDGF-BB: 24 kDa, ²⁰² VEGF-A: 45 kDa. ²⁰³

Trafficking kinetics

Trafficking parameters were determined by fitting to experimental data (ESI,† Fig. S1 and Table 2)^{171,172,204–207} encompassing multiple receptor and cell types to decouple cell- or receptor-specific trafficking mechanisms, and define generalized trafficking kinetics. Note that the receptor types used in this fitting were limited by availability of experimental data; as such, some of the experimental receptor types differ from the eight RTKs we study here (receptor types used for fitting are ICAM-1, 172,204 VEGFR2, 205 EGFR²⁰⁶ and heparin sulfate and integrins¹⁷¹). We assume this discrepancy is negligible, as we use this fitting approach to decouple receptor-specific trafficking mechanisms and define generalized trafficking parameters, as stated. Such an approach using generalized trafficking parameters is a typical computational modeling assumption 32,37,160,173,208,209 that retains physiological relevancy. For example, Tan et al. modeled VEGFR2 internalization with generalized trafficking kinetics, while still accurately predicting VEGFR2 and ERK phosphorylation dynamics. 159 Trafficking kinetics were defined by minimizing the global Chi-square between experimental data and simulation:

$$\min \left[\sum_{i=1}^{n} \frac{(\bar{y}_i - \hat{y}_i)^2}{\bar{y}_i} \right] \tag{5}$$

where \bar{y}_i is the mean value of experimental data point i, \hat{y}_i is the simulated value and n is the total number of experimental data points. Best fit trafficking parameters were determined using 10 000 Monte Carlo simulations for each of the eight RTKs (*i.e.* RTK specific receptor/ligand concentrations and interaction kinetics); the best fit parameters were then represented

Integrative Biology Paper

as the mean \pm standard deviation across these eight RTKs (Table 2). Each Monte Carlo simulation seeded the trafficking parameters between 1×10^{-7} and 1×10^{-1} and calculated the Chi-square between simulation and experiment (eqn (5)); this parameter range represents one order of magnitude lower and higher than trafficking kinetic rates used in other physiological models. 37,160,210,211 Experimental data are provided throughout the entire trafficking process, including membrane internalization (Fig. S1A, ESI†), nuclear translocated receptors (Fig. S1B, ESI†), endosome receptors (Fig. S1C and D, ESI†) and lysosome receptors (Fig. S1E and F, ESI†). While experimental data for compartments other than membrane, early endosome, lysosome, and nucleus were not available, we assume that by accurately fitting receptor localization to these compartments, receptor localization in the other compartments will also be accurate. Indeed, the compartments without experimental definition: endocytic vesicles, recycling endosomes, and late endosomes, are all compartments intermediary to compartments with experimental data. Thus, we assume that accurately fitting membrane and early endosome localization will implicitly fit endocytic vesicle localization, which occurs in between these two compartments, accurately.

Simulating RTK signaling with Monte Carlo

For all simulations examining RTK trafficking and compartmentalized RTK signaling (Fig. 2, 4 and 5), the range of possible RTK signaling was determined through Monte Carlo simulations. For each Monte Carlo simulation, the 20 trafficking parameters were randomly seeded from the range provided by their mean \pm standard deviation (Table 2). Using those 20 random trafficking parameters, the compartmentalized RTK signaling was simulated; this random seeding and simulation was performed 10 000 times. The results from the 10 000 simulations were then aggregated as mean \pm standard deviation to create the range of compartmentalized RTK signaling as given (Fig. 2, 4 and 5).

Acknowledgements

We would like to acknowledge Spencer Mamer, Si Chen and Ali Ansari for many helpful discussions with model building and data representation. This work was supported in part by grants from the American Cancer Society (282802), National Science Foundation (1512598) and American Heart Association (16SDG26940002).

References

- 1 N. E. Hynes and H. A. Lane, Nat. Rev. Cancer, 2005, 5, 341-354.
- 2 M. Niepel, M. Hafner, E. A. Pace, M. Chung, D. H. Chai, L. Zhou, B. Schoeberl and P. K. Sorger, Sci. Signaling, 2013,
- 3 E. Murphy, Circ. Res., 2011, 109, 687-696.
- 4 S. Wassmann and G. Nickenig, J. Hypertens Suppl., 2006, 24, S15-S21.

- 5 I. J. Uings and S. N. Farrow, Mol. Pathol., 2000, 53, 295-299.
- 6 M. A. Lemmon and J. Schlessinger, Cell, 2010, 141, 1117-1134.
- 7 I. N. Maruyama, Cells, 2014, 3, 304.
- 8 P. Seshacharyulu, M. P. Ponnusamy, D. Haridas, M. Jain, A. Ganti and S. K. Batra, Expert Opin. Ther. Targets, 2012, **16**, 15-31.
- 9 N. Kabbani, Proteomics, 2008, 8, 4146-4155.
- 10 M. Arish, A. Husein, M. Kashif, P. Sandhu, S. E. Hasnain, Y. Akhter and A. Rub, Biochimie, 2015, 113, 111-124.
- 11 A. Sorkin and M. von Zastrow, Nat. Rev. Mol. Cell Biol., 2002, 3, 600-614.
- 12 D. A. Lauffenburger and J. Linderman, Receptors: Models for Binding, Trafficking, and Signaling, 1993.
- 13 C. Le Roy and J. L. Wrana, Nat. Rev. Mol. Cell Biol., 2005, 6,
- 14 S. Mukherjee, Circ. Res., 2006, 98, 743-756.
- 15 M. Pálfy, A. Reményi and T. Korcsmáros, Trends Cell Biol., 2015, 22, 447-456.
- 16 H. Kitano, Nature, 2002, 420, 206-210.
- 17 M. Miaczynska, L. Pelkmans and M. Zerial, Curr. Opin. Cell Biol., 2004, 16, 400-406.
- 18 R. Irannejad, N. G. Tsvetanova, B. T. Lobingier and M. von Zastrow, Curr. Opin. Cell Biol., 2015, 35, 137-143.
- 19 H. S. Wiley, J. J. Herbst, B. J. Walsh, D. A. Lauffenburger, M. G. Rosenfeld and G. N. Gill, J. Biol. Chem., 1991, 266, 11083-11094.
- 20 A. Ciechanover, A. L. Schwartz, A. Dautry-Varsat and H. F. Lodish, J. Biol. Chem., 1983, 258, 16-9681.
- 21 C. M. Waters, K. C. Oberg, G. Carpenter and K. A. Overholser, Biochemistry, 1990, 29, 3563-3569.
- 22 D. A. Lauffenburger, J. Linderman and L. Berkowitz, Ann. N. Y. Acad. Sci., 1987, 506, 147-162.
- 23 J. J. Linderman and D. A. Lauffenburger, Receptor/Ligand Sorting Along the Endocytic Pathway, 1989.
- 24 G. M. Di Guglielmo, P. C. Baass, W. J. Ou, B. I. Posner and J. J. Bergeron, EMBO J., 1994, 13, 4269–4277.
- 25 A. Tomas, C. E. Futter and E. R. Eden, Trends Cell Biol., 2015, 24, 26-34.
- 26 H. W. Platta and H. Stenmark, Curr. Opin. Cell Biol., 2011, 23, 393-403.
- 27 M. Simons, Physiology, 2012, 27, 213-222.
- 28 S. Mittar, C. Ulyatt, G. J. Howell, A. F. Bruns, I. Zachary, J. H. Walker and S. Ponnambalam, Exp. Cell Res., 2009, 315, 877-889.
- 29 Z. Zhang, K. G. Neiva, M. W. Lingen, L. M. Ellis and J. E. Nor, Cell Death Differ., 2010, 17, 499-512.
- 30 B. Mezquita, J. Mezquita, M. Pau and C. Mezquita, J. Cell. Biochem., 2010, 110, 732-742.
- 31 A.-M. Chioni and R. Grose, J. Cell Biol., 2012, 197, 801-817.
- 32 L. W. Clegg and F. Mac Gabhann, PLoS Comput. Biol., 2015, 11, e1004158.
- 33 T. Matsumoto, S. Bohman, J. Dixelius, T. Berge, A. Dimberg, P. Magnusson, L. Wang, C. Wikner, J. H. Qi, C. Wernstedt, J. Wu, S. Bruheim, H. Mugishima, D. Mukhopadhyay, A. Spurkland and L. Claesson-Welsh, EMBO J., 2005, 24, 2342-2353.

- 34 J. Tong, P. Taylor, S. M. Peterman, A. Prakash and M. F. Moran, *Mol. Cell. Proteomics*, 2009, **8**, 2131–2144.
- 35 Y.-W. Chang, C.-M. Su, Y.-H. Su, Y.-S. Ho, H.-H. Lai, H.-A. Chen, M.-L. Kuo, W.-C. Hung, Y.-W. Chen, C.-H. Wu, P.-S. Chen and J.-L. Su, *Oncotarget*, 2014, 5, 3823–3835.
- 36 T. Maretzky, A. Evers, W. Zhou, S. L. Swendeman, P.-M. Wong, S. Rafii, K. Reiss and C. P. Blobel, *Nat. Commun.*, 2011, 2, 229.
- 37 B. Schoeberl, C. Eichler-Jonsson, E. D. Gilles and G. Muller, *Nat. Biotechnol.*, 2002, **20**, 370–375.
- 38 S. Chen, X. Guo, O. Imarenezor and P. Imoukhuede, *Cell. Mol. Bioeng.*, 2015, **8**, 383–403.
- 39 L. Comps-Agrar, D. R. Dunshee, D. L. Eaton and J. Sonoda, J. Biol. Chem., 2015, 290, 24166–24177.
- 40 A. O'Neill, N. Shah, N. Zitomersky, M. Ladanyi, N. Shukla, A. Uren, D. Loeb and J. Toretsky, *Sarcoma*, 2013, 2013, 450478.
- 41 S. Chen, J. Weddell, P. Gupta, G. Conard, J. Parkin and P. I. Imoukhuede, qFlow Cytometry-Based Receptoromic Screening: A High-Throughput Quantification Approach Informing Biomarker Selection and Nanosensor Development, in *Biomedical Nanotechnology: Methods and Protocols*, ed. S. H. Petrosko and E. S. Day, Springer New York, New York, NY, 2017, pp. 117–138.
- 42 S. D. Finley, M. O. Engel-Stefanini, P. Imoukhuede and A. S. Popel, *BMC Syst. Biol.*, 2011, 5, 193.
- 43 O. A. Ibrahimi, F. Zhang, S. C. Lang Hrstka, M. Mohammadi and R. J. Linhardt, *Biochemistry*, 2004, 43, 4724-4730.
- 44 B. E. Forbes, P. J. Hartfield, K. A. McNeil, K. H. Surinya, S. J. Milner, L. J. Cosgrove and J. C. Wallace, *Eur. J. Biochem.*, 2002, 269, 961–968.
- 45 W. Hu, J. Kumar, C. Huang and W. Chen, *BioMed Res. Int.*, 2015, 2015, 8.
- 46 D. Kumar, R. Srikanth, H. Ahlfors, R. Lahesmaa and K. V. S. Rao, *Mol. Syst. Biol.*, 2007, 3, 150.
- 47 M. Schilling, T. Maiwald, S. Hengl, D. Winter, C. Kreutz, W. Kolch, W. D. Lehmann, J. Timmer and U. Klingmüller, Mol. Syst. Biol., 2009, 5, 334.
- 48 J. W. Locasale, BMC Syst. Biol., 2008, 2, 1-11.
- 49 D. Wang and M. W. Quick, *J. Biol. Chem.*, 2005, **280**, 18703–18709.
- 50 R. Villaseñor, H. Nonaka, P. Del Conte-Zerial, Y. Kalaidzidis and M. Zerial, *eLife*, 2015, 4, e06156.
- 51 H. J. Geuze, J. W. Slot and A. L. Schwartz, J. Cell Biol., 1987, 104, 1715–1723.
- 52 E. Zwick, J. Bange and A. Ullrich, Endocr.-Relat. Cancer, 2001, 8, 161–174.
- 53 K. Takeuchi and F. Ito, *Biol. Pharm. Bull.*, 2011, 34, 1774–1780.
- 54 T. Kitazono, S. Ibayashi, T. Nagao, T. Kagiyama, J. Kitayama and M. Fujishima, *Stroke*, 1998, **29**, 494–498.
- 55 I. Gagalo, I. Rusiecka and I. Kocic, *Curr. Neuropharmacol.*, 2016, **13**, 836–844.
- 56 S. V. Costes, I. Chiolo, J. M. Pluth, M. H. Barcellos-Hoff and B. Jakob, *Mutat. Res.*, 2010, **704**, 78–87.

- 57 J. Rink, E. Ghigo, Y. Kalaidzidis and M. Zerial, *Cell*, 2005, 122, 735–749.
- 58 R. Fernandez-Gonzalez, M. H. Barcellos-Hoff and C. Ortiz-de-Solorzano, *IEEE Trans. Image Process*, 2005, 14, 1300–1313.
- 59 V. Zinchuk, Y. Wu and O. Grossenbacher-Zinchuk, Sci. Rep., 2013, 3, 1365.
- 60 I. L. Arancibia-Carcamo, B. P. Fairfax, S. J. Moss and J. T. Kittler, *The Dynamic Synapse: Molecular Methods in Ionotropic Receptor Biology*, 2006, p. chapter 6.
- 61 M. Jovic, M. Sharma, J. Rahajeng and S. Caplan, *Histol. Histopathol.*, 2010, 25, 99–112.
- 62 K. W. Dunn, M. M. Kamocka and J. H. McDonald, Am. J. Physiol.: Cell Physiol., 2011, 300, C723-C742.
- 63 W. H. Humphries IV, C. J. Szymanski and C. K. Payne, *PLoS One*, 2011, **6**, e26626.
- 64 L. Stokes, Purinergic Signalling, 2013, 9, 113-121.
- 65 P. C. Baass, G. M. Di Guglielmo, F. Authier, B. I. Posner and J. J. M. Bergeron, *Trends Cell Biol.*, 1995, 5, 465–470.
- 66 P. Burke, K. Schooler and H. S. Wiley, *Mol. Biol. Cell*, 2001, 12, 1897–1910.
- 67 Y. Wang, S. D. Pennock, X. Chen, A. Kazlauskas and Z. Wang, J. Biol. Chem., 2004, 279, 8038–8046.
- 68 H. M. Jopling, A. F. Odell, N. M. Hooper, I. C. Zachary, J. H. Walker and S. Ponnambalam, *Arterioscler., Thromb.*, *Vasc. Biol.*, 2009, 29, 1119–1124.
- 69 P. Sharma, A. Chawla and P. Pawar, Sci. World J., 2013, 654829.
- 70 R. Siegel and M. Rathbone, in *Fundamentals and Applications of Controlled Release Drug DeliverySE-2*, ed. J. Siepmann, R. A. Siegel and M. J. Rathbone, Springer US, 2012, pp. 19–43.
- 71 Y. Fu and W. J. Kao, Expert Opin. Drug Delivery, 2010, 7, 429–444.
- 72 S. Moens, J. Goveia, P. C. Stapor, A. R. Cantelmo and P. Carmeliet, *Cytokine Growth Factor Rev.*, 2014, **25**, 473–482.
- 73 G. McMahon, Oncologist, 2000, 5, 3-10.
- 74 H. M. Jopling, G. J. Howell, N. Gamper and S. Ponnambalam, *Biochem. Biophys. Res. Commun.*, 2011, **410**, 170–176.
- 75 P. I. Imoukhuede and A. S. Popel, *PLoS One*, 2012, 7, e44791.
- 76 R. L. Juliano, X. Ming, K. Carver and B. Laing, *Nucleic Acid Ther.*, 2014, 24, 101–113.
- 77 P. D. Dobson and D. B. Kell, *Nat. Rev. Drug Discovery*, 2008,7, 205–220.
- 78 A. Wicki, C. Rochlitz, A. Orleth, R. Ritschard, I. Albrecht, R. Herrmann, G. Christofori and C. Mamot, *Clin. Cancer Res.*, 2012, 18, 454–464.
- 79 J. A. Allen, R. A. Halverson-Tamboli and M. M. Rasenick, *Nat. Rev. Neurosci.*, 2007, **8**, 128–140.
- 80 D. Locke, H. Chen, Y. Liu, C. Liu and M. L. Kahn, J. Biol. Chem., 2002, 277, 18801–18809.
- 81 L. J. Bugaj, D. P. Spelke, C. K. Mesuda, M. Varedi, R. S. Kane and D. V. Schaffer, *Nat. Commun.*, 2015, **6**, 6898.
- 82 A. V. Vieira, C. Lamaze and S. L. Schmid, *Science*, 1996, **274**, 2086–2089.
- 83 G. Auciello, D. L. Cunningham, T. Tatar, J. K. Heath and J. Z. Rappoport, *J. Cell Sci.*, 2013, **126**, 613–624.

84 A. S. Martins, J. L. Ordonez, A. T. Amaral, F. Prins, G. Floris, M. Debiec-Rychter, P. C. W. Hogendoorn and

Integrative Biology

- G. Floris, M. Debiec-Rychter, P. C. W. Hogendoorn and E. de Alava, *PLoS One*, 2011, **6**, e19846.
- 85 M. Huang, J. B. DuHadaway, G. C. Prendergast and L. D. Laury-Kleintop, *Arterioscler., Thromb., Vasc. Biol.*, 2007, 27, 2597–2605.
- 86 A. A. Lanahan, K. Hermans, F. Claes, J. S. Kerley-Hamilton, Z. W. Zhuang, F. J. Giordano, P. Carmeliet and M. Simons, *Dev. Cell*, 2010, 18, 713–724.
- 87 D. Chen, D. Zuo, C. Luan, M. Liu, M. Na, L. Ran, Y. Sun, A. Persson, E. Englund, L. G. Salford, E. Renström, X. Fan and E. Zhang, *PLoS One*, 2014, **9**, e87281.
- 88 Y. Nishimura, B. Bereczky and M. Ono, *Histochem. Cell Biol.*, 2007, **127**, 541–553.
- 89 Y. Nishimura, K. Yoshioka, B. Bereczky and K. Itoh, *Mol. Cancer*, 2008, 7, 42.
- 90 D. K. Giri, M. Ali-Seyed, L.-Y. Li, D.-F. Lee, P. Ling, G. Bartholomeusz, S.-C. Wang and M.-C. Hung, *Mol. Cell. Biol.*, 2005, 25, 11005–11018.
- 91 H.-W. Lo, M. Ali-Seyed, Y. Wu, G. Bartholomeusz, S.-C. Hsu and M.-C. Hung, *J. Cell. Biochem.*, 2006, **98**, 1570–1583.
- 92 Y. N. Wang, H. Yamaguchi, J. M. Hsu and M. C. Hung, *Oncogene*, 2010, **29**, 3997–4006.
- 93 G. Carpenter and H.-J. Liao, *Cold Spring Harbor Perspect. Biol.*, 2013, 5, a008979.
- 94 M. B. Hossain, N. Cortes-Santiago, X. Fan, K. Gabrusiewicz, J. Gumin, E. P. Sulman, F. Lang, R. Sawaya, W. K. A. Yung, J. Fueyo and C. Gomez-Manzano, *Cancer Res.*, 2014, 74, 3944.
- 95 M. B. Hossain, R. Shifat, D. G. Johnson, M. T. Bedford, K. R. Gabrusiewicz, N. Cortes-Santiago, X. Luo, R. Ezhilarasan, E. P. Sulman, H. Jiang, S. S. C. Li, F. F. Lang, J. Tyler, M. Hung, J. Fueyo and C. Gomez-Manzano, *Cell Biol.*, 2016, 2, e1501290.
- 96 S.-Y. Lin, K. Makino, W. Xia, A. Matin, Y. Wen, K. Y. Kwong, L. Bourguignon and M.-C. Hung, *Nat. Cell Biol.*, 2001, 3, 802–808.
- 97 G. Liccardi, J. A. Hartley and D. Hochhauser, *Cancer Res.*, 2011, 71, 1103–1114.
- 98 W.-C. Huang, Y.-J. Chen, L.-Y. Li, Y.-L. Wei, S.-C. Hsu, S.-L. Tsai, P.-C. Chiu, W.-P. Huang, Y.-N. Wang, C.-H. Chen, W.-C. Chang, W.-C. Chang, A. J.-E. Chen, C.-H. Tsai and M.-C. Hung, J. Biol. Chem., 2011, 286, 20558–20568.
- 99 P. A. Maher, J. Cell Biol., 1996, 134, 529-536.
- 100 M. K. Stachowiak, P. A. Maher, A. Joy, E. Mordechai and E. K. Stachowiak, *Mol. Biol. Cell*, 1996, 7, 1299–1317.
- 101 J. F. Reilly and P. A. Maher, J. Cell Biol., 2001, 152, 1307-1312.
- 102 C.-W. Chen and D. Roy, Mol. Cell. Endocrinol., 1996, 118, 1-8.
- 103 B. Sehat, A. Tofigh, Y. Lin, E. Trocmé, U. Liljedahl, J. Lagergren and O. Larsson, *Sci. Signaling*, 2010, 3, ra10.
- 104 T. Aleksic, M. M. Chitnis, O. V. Perestenko, S. Gao, P. H. Thomas, G. D. Turner, A. S. Protheroe, M. Howarth and V. M. Macaulay, *Cancer Res.*, 2010, 70, 6412–6419.
- 105 H. Deng, Y. Lin, M. Badin, D. Vasilcanu, T. Strömberg, H. Jernberg-Wiklund, B. Sehat and O. Larsson, *Biochem. Biophys. Res. Commun.*, 2011, 404, 667–671.

- 106 M. I. Aslam, S. Hettmer, J. Abraham, D. LaTocha, A. Soundararajan, E. T. Huang, M. W. Goros, J. E. Michalek, S. Wang, A. Mansoor, B. J. Druker, A. J. Wagers, J. W. Tyner and C. Keller, *Mol. Cancer Res.*, 2013, 11, 1303–1313.
- 107 B. A. Lee, D. W. Maher, M. Hannink and D. J. Donoghue, Mol. Cell. Biol., 1987, 7, 3527–3537.
- 108 J. Cai, W. G. Jiang, M. B. Grant and M. Boulton, J. Biol. Chem., 2006, 281, 3604–3613.
- 109 T.-H. Lee, S. Seng, M. Sekine, C. Hinton, Y. Fu, H. K. Avraham and S. Avraham, *PLoS Med.*, 2007, 4, e186.
- 110 S. C. R. Santos and S. Dias, Blood, 2004, 103, 3883-3889.
- 111 S. B. Fox, H. Turley, M. Cheale, C. Blázquez, H. Roberts, N. James, N. Cook, A. Harris and K. Gatter, *J. Pathol.*, 2004, 202, 313–320.
- 112 M. Stewart, H. Turley, N. Cook, F. Pezzella, G. Pillai, D. Ogilvie, S. Cartlidge, D. Paterson, C. Copley, J. Kendrew, C. Barnes, A. L. Harris and K. C. Gatter, *Histopathology*, 2003, 43, 33–39.
- 113 Y. Zhang, G. Pillai, K. Gatter, C. Blázquez, H. Turley, F. Pezzella and S. M. Watt, *Hum. Pathol.*, 2005, **36**, 797–805.
- 114 I. Domingues, J. Rino, J. A. A. Demmers, P. de Lanerolle and S. C. R. Santos, *PLoS One*, 2011, **6**, e25668.
- 115 L. Johannes and V. Popoff, Cell, 2008, 135, 1175-1187.
- 116 R. A. Spooner, D. C. Smith, A. J. Easton, L. M. Roberts and J. M. Lord, *Virol. J.*, 2006, 3, 26.
- 117 K. Sandvig and B. van Deurs, *Annu. Rev. Cell Dev. Biol.*, 2002, **18**, 1–24.
- 118 M. K. Chen and M. C. Hung, FEBS J., 2015, 282, 3693-3721.
- 119 E. Rovida and P. Dello Sbarba, *Cell. Mol. Life Sci.*, 2014, **71**, 3627–3631.
- 120 S. C. Wang, H.-C. Lien, W. Xia, I.-F. Chen, H.-W. Lo, Z. Wang, M. Ali-Seyed, D.-F. Lee, G. Bartholomeusz, F. Ou-Yang, D. K. Giri and M.-C. Hung, *Cancer Cell*, 2004, 6, 251–261.
- 121 C. C. Williams, J. G. Allison, G. A. Vidal, M. E. Burrow, B. S. Beckman, L. Marrero and F. E. Jones, *J. Cell Biol.*, 2004, **167**, 469–478.
- 122 L. K. Goh and A. Sorkin, *Cold Spring Harbor Perspect. Biol.*, 2013, 5, a017459.
- 123 D. Padrón, M. Sato, J. W. Shay, A. F. Gazdar, J. D. Minna and M. G. Roth, *Cancer Res.*, 2007, **67**, 7695–7702.
- 124 J. C. Weddell and P. I. Imoukhuede, *Encycl. Cardiovasc. Res. Med.*, 2017, accepted.
- 125 J. N. Bazil, G. T. Buzzard and A. E. Rundell, *Bull. Math. Biol.*, 2012, **74**, 688.
- 126 J. C. Weddell and P. I. Imoukhuede, *PLoS One*, 2014, 9, e97271.
- 127 J. C. Weddell, S. Chen and P. I. Imoukhuede, *Nat. Sys. Biol. Appl.*, 2017, in review.
- 128 S. Chen, J. Weddell, P. Gupta, G. Conard, J. Parkin and P. I. Imoukhuede, qFlow Cytometry-Based Receptoromic Screening: A High-Throughput Quantification Approach Informing Biomarker Selection and Nanosensor Development, in *Biomedical Nanotechnology: Methods and Protocols*, ed. S. H. Petrosko and E. S. Day, Springer New York, New York, NY, 2017, pp. 117–138.

- 129 L.-H. Chu, V. C. Ganta, M. H. Choi, G. Chen, S. D. Finley, B. H. Annex and A. S. Popel, *Sci. Rep.*, 2016, **6**, 37030.
- 130 S. D. Finley, P. Angelikopoulos, P. Koumoutsakos and A. S. Popel, *CPT: Pharmacometrics Syst. Pharmacol.*, 2015, 4, 641–649.
- 131 K.-A. Norton, A. S. Popel and N. B. Pandey, *Am. J. Cancer Res.*, 2015, 5, 1295–1307.
- 132 P. I. Imoukhuede, A. O. Dokun, B. H. Annex and A. S. Popel, *Am. J. Physiol.: Heart Circ. Physiol.*, 2013, **304**, H1085–H1093.
- 133 P. I. Imoukhuede and A. S. A. Popel, Exp. Cell Res., 2011, 317, 955–965.
- 134 P. I. Imoukhuede and A. S. Popel, *Cancer Med.*, 2014, 3, 225–244.
- 135 K. Kisler, R. H. Chow and R. Dominguez, *J. Steroids Horm. Sci.*, 2013, Suppl 12.
- 136 N. F. Neel, E. Schutyser, J. Sai, G.-H. Fan and A. Richmond, *Cytokine Growth Factor Rev.*, 2005, **16**, 637–658.
- 137 E. Macia, M. Ehrlich, R. Massol, E. Boucrot, C. Brunner and T. Kirchhausen, *Dev. Cell*, 2006, **10**, 839–850.
- 138 N. Signoret, J. Oldridge, A. Pelchen-Matthews, P. J. Klasse, T. Tran, L. F. Brass, M. M. Rosenkilde, T. W. Schwartz, W. Holmes, W. Dallas, M. A. Luther, T. N. C. Wells, J. A. Hoxie and M. Marsh, J. Cell Biol., 1997, 139, 651–664.
- 139 N. García-Tardón, I. M. González-González, J. Martínez-Villarreal, E. Fernández-Sánchez, C. Giménez and F. Zafra, J. Biol. Chem., 2012, 287, 19177–19187.
- 140 A. Aballay, P. D. Stahl and L. S. Mayorga, J. Cell Sci., 1999, 112(pt 1), 2549–2557.
- 141 L. Rodriguez, C. J. Stirling and P. G. Woodman, *Mol. Biol. Cell*, 1994, 5, 773–783.
- 142 A. T. Jones and M. Wessling-Resnick, *J. Biol. Chem.*, 1998, 273, 25301–25309.
- 143 H. M. Jopling, A. F. Odell, N. M. Hooper, I. C. Zachary, J. H. Walker and S. Ponnambalam, *Arterioscler., Thromb., Vasc. Biol.*, 2009, **29**, 1119–1124.
- 144 B. a. Mainou and T. S. Dermody, *J. Virol.*, 2012, **86**, 8346–8358.
- 145 A. H. Hutagalung and P. J. Novick, *Physiol. Rev.*, 2011, 91, 119–149.
- 146 B. P. Ceresa, *Histol. Histopathol.*, 2006, **21**, 987–993.
- 147 A. T. Krueger, C. Kroll, E. Sanchez, L. G. Griffith and B. Imperiali, *Angew. Chem., Int. Ed.*, 2014, 53, 2662–2666.
- 148 X. Ye, Y. Abou-Rayyah, J. Bischoff, A. Ritchie, N. J. Sebire, P. Watts, A. J. Churchill and D. O. Bates, *J. Pathol.*, 2016, 239, 139–151.
- 149 A. Laperle, K. S. Masters and S. P. Palecek, *Biotechnol. Prog.*, 2015, **31**, 212–219.
- 150 Y. Goyal, G. A. Jindal, J. L. Pelliccia, K. Yamaya, E. Yeung, A. S. Futran, R. D. Burdine, T. Schupbach and S. Y. Shvartsman, *Nat. Genet.*, 2017, 49, 465–469.
- 151 C. I. Stains, N. C. Tedford, T. C. Walkup, E. Luković, B. N. Goguen, L. G. Griffith, D. A. Lauffenburger and B. Imperiali, *Chem. Biol.*, 2012, 19, 210–217.
- 152 S. Dayalan Naidu, C. Sutherland, Y. Zhang, A. Risco, L. de la Vega, C. J. Caunt, C. J. Hastie, D. J. Lamont, L. Torrente,

- S. Chowdhry, I. J. Benjamin, S. M. Keyse, A. Cuenda and A. T. Dinkova-Kostova, *Mol. Cell. Biol.*, 2016, **36**, 2403–2417.
- 153 M. A. Miller, M. J. Oudin, R. J. Sullivan, S. J. Wang, A. S. Meyer, H. Im, D. T. Frederick, J. Tadros, L. G. Griffith, H. Lee, R. Weissleder, K. T. Flaherty, F. B. Gertler and D. A. Lauffenburger, *Cancer Discovery*, 2016, 6, 382–399.
- 154 T. Umezu, K. Ohyashiki, M. Kuroda and J. H. Ohyashiki, *Oncogene*, 2013, 32, 2747–2755.
- 155 H. Klingberg, L. B. Oddershede, K. Loeschner, E. H. Larsen, S. Loft and P. Møller, *Toxicol. Res.*, 2015, 4, 655–666.
- 156 J. G. Lock and J. L. Stow, *Mol. Biol. Cell*, 2005, **16**, 1744–1755.
- 157 D. Poteryaev, S. Datta, K. Ackema, M. Zerial and A. Spang, *Cell*, 2010, **141**, 497–508.
- 158 B. N. Kholodenko, Nat. Rev. Mol. Cell Biol., 2006, 7, 165–176.
- 159 W. H. Tan, A. S. Popel and F. Mac Gabhann, *PLoS One*, 2013, **8**, e67438.
- 160 W. H. Tan, A. S. Popel and F. Mac Gabhann, *Cell. Signalling*, 2013, 25, 2496–2510.
- 161 F. Mac Gabhann and A. S. Popel, *Biophys. Chem.*, 2007, **128**, 125–139.
- 162 S. Y. Shvartsman, C. B. Muratov and D. A. Lauffenburger, Development, 2002, 129, 2577–2589.
- 163 D. M. Freed, D. Alvarado and M. A. Lemmon, *Nat. Commun.*, 2015, 6, 7380.
- 164 T. Moriki, H. Maruyama and I. N. Maruyama, *J. Mol. Biol.*, 2001, 311, 1011–1026.
- 165 B. Schuster, W. Meinert, S. Rose-John and K.-J. Kallen, *FEBS Lett.*, 2003, **538**, 113–116.
- 166 S. Sarabipour, K. Ballmer-Hofer and K. Hristova, *eLife*, 2016, **5**, e13876.
- 167 C. Ruch, G. Skiniotis, M. O. Steinmetz, T. Walz and K. Ballmer-Hofer, *Nat. Struct. Mol. Biol.*, 2007, **14**, 249–250.
- 168 B. S. Hendriks, J. Cook, J. M. Burke, D. A. Beusmans, J. M. Lauffenburger and D. de Graaf, Syst. Biol., 2006, 153, 22–33.
- 169 E. M. Fallon and D. A. Lauffenburger, *Biotechnol. Prog.*, 2000, **16**, 905–916.
- 170 A. R. Gallimore, A. R. Aricescu, M. Yuzaki and R. Calinescu, *PLoS Comput. Biol.*, 2016, 12, e1004664.
- 171 W. Greene, W. Zhang, M. He, C. Witt, F. Ye and S.-J. Gao, *PLoS Pathog.*, 2012, **8**, e1002703.
- 172 S. Muro, C. Gajewski, M. Koval and V. R. Muzykantov, *Blood*, 2004, **105**, 650–658.
- 173 A. R. French and D. A. Lauffenburger, *Ann. Biomed. Eng.*, 1997, 25, 690–707.
- 174 R. Lundmark and S. R. Carlsson, *Semin. Cell Dev. Biol.*, 2010, 21, 363-370.
- 175 N. Ben-Dov and R. Korenstein, *Biochim. Biophys. Acta, Biomembr.*, 2013, **1828**, 2672–2681.
- 176 R. C. Aguilar and B. Wendland, Proc. Natl. Acad. Sci. U. S. A., 2005, 102, 2679–2680.
- 177 S. McLaughlin and D. Murray, Nature, 2005, 438, 605-611.
- 178 G. Di Paolo and P. De Camilli, *Nature*, 2006, 443, 651-657.

Published on 12 April 2017. Downloaded by University of Illinois - Urbana on 09/05/2017 22:09:36.

Integrative Biology

179 S. Funamoto, R. Meili, S. Lee, L. Parry and R. A. Firtel, *Cell*, 2002, **109**, 611–623.

- 180 X. Gao, P. R. Lowry, X. Zhou, C. Depry, Z. Wei, G. W. Wong and J. Zhang, *Proc. Natl. Acad. Sci. U. S. A.*, 2011, **108**, 14509–14514.
- 181 Y. Mosesson, G. B. Mills and Y. Yarden, *Nat. Rev. Cancer*, 2008, **8**, 835–850.
- 182 H. Lodish, A. Berk, S. L. Zipursky, P. Matsudaira, D. Baltimore and J. Darnell, *Molecular Cell Biology*, 2000, p. section 17.9.
- 183 J. P. Luzio, P. R. Pryor and N. A. Bright, *Nat. Rev. Mol. Cell Biol.*, 2007, **8**, 622–632.
- 184 Corning, Surface Areas and Recommend Volumes for Corning[®] Cell Culture Vessels, 2008.
- 185 R. C. Molden, J. Goya, Z. Khan and B. A. Garcia, *Mol. Cell. Proteomics*, 2014, **13**, 1106–1118.
- 186 L. B. Kleiman, T. Maiwald, H. Conzelmann, D. A. Lauffenburger and P. K. Sorger, *Mol. Cell*, 2011, 43, 723–737.
- 187 S. C. D. van IJzendoorn, J. Cell Sci., 2006, 119, 1679-1681.
- 188 G. R. Bright, G. W. Fisher, J. Rogowska and D. L. Taylor, *J. Cell Biol.*, 1987, **104**, 1019–1033.
- 189 K. Maeda, Y. Kato and Y. Sugiyama, *J. Controlled Release*, 2002, **82**, 71–82.
- 190 K. Ek and P. G. Righetti, Electrophoresis, 1980, 1, 137-140.
- 191 A. R. French, D. K. Tadaki, S. K. Niyogi and D. A. Lauffenburger, *J. Biol. Chem.*, 1995, **270**, 4334–4340.
- 192 M. Nunez, K. H. Mayo, C. Starbuck and D. Lauffenburger, J. Cell. Biochem., 1993, 51, 312–321.
- 193 R. Ebner and R. Derynck, Cell Regul., 1991, 2, 599-612.
- 194 J. L. Newsted and J. P. Giesy, Gen. Comp. Endocrinol., 1991, 83, 345–353.
- 195 C. A. Sarkar, K. Lowenhaupt, T. Horan, T. C. Boone, B. Tidor and D. A. Lauffenburger, *Nat. Biotechnol.*, 2002, 20, 908–913.
- 196 P. H. Hinderling and D. Hartmann, *Ther. Drug Monit.*, 2005, 27, 71–85.
- 197 J. Llopis, J. M. McCaffery, A. Miyawaki, M. G. Farquhar and R. Y. Tsien, *Proc. Natl. Acad. Sci. U. S. A.*, 1998, 95, 6803–6808.
- 198 Z. L. Zhang, J. F. Zhang, Y. F. Yuan, Y. M. He, Q. Y. Liu, X. W. Mao, Y. B. Ai and Z. S. Liu, *Exp. Ther. Med.*, 2014, 7, 543–552.
- 199 J. M. Taylor, S. Cohen and W. M. Mitchell, *Proc. Natl. Acad. Sci. U. S. A.*, 1970, **67**, 164–171.
- 200 K. Chlebova, V. Bryja, P. Dvorak, A. Kozubik, W. R. Wilcox and P. Krejci, *Cell. Mol. Life Sci.*, 2009, **66**, 225–235.
- 201 E. Rinderknecht and R. E. Humbel, *J. Biol. Chem.*, 1978, 253, 2769–2776.
- 202 A. Ostman, J. Thyberg, B. Westermark and C. H. Heldin, J. Cell Biol., 1992, 118, 509–519.

- 203 M. O. Stefanini, F. T. Wu, F. Mac Gabhann and A. S. Popel, BMC Syst. Biol., 2008, 2, 77.
- 204 S. Muro, X. Cui, C. Gajewski, J.-C. Murciano, V. R. Muzykantov and M. Koval, Am. J. Physiol.: Cell Physiol., 2003, 285, C1339–C1347.
- 205 M. G. Lampugnani, F. Orsenigo, M. C. Gagliani, C. Tacchetti and E. Dejana, J. Cell Biol., 2006, 174, 593–604.
- 206 L. Danglot, M. Chaineau, M. Dahan, M.-C. Gendron, N. Boggetto, F. Perez and T. Galli, J. Cell Sci., 2010, 123, 723-735.
- 207 S. Iadevaia, Y. Lu, F. C. Morales, G. B. Mills and P. T. Ram, Cancer Res., 2010, 70, 6704–6714.
- 208 M. Sumit, R. R. Neubig, S. Takayama and J. J. Linderman, *Integr. Biol.*, 2015, 7, 1378–1386.
- 209 S. M. Anderson, B. Shergill, Z. T. Barry, E. Manousiouthakis, T. T. Chen, E. Botvinick, M. O. Platt, M. L. Iruela-Arispe and T. Segura, *Integr. Biol.*, 2011, 3, 887–896.
- 210 C. S. Monast, C. M. Furcht and M. J. Lazzara, *Biophys. J.*, 2012, **102**, 2012–2021.
- 211 B. S. Hendriks, L. K. Opresko, H. S. Wiley, H. E. R. O. Effects and D. Lauffenburger, *Cancer Res.*, 2003, 2, 1130–1137.
- 212 T. Annussek, T. Szuwart, J. Kleinheinz, C. Koiky and K. Wermker, *Head Face Med.*, 2014, **10**, 19.
- 213 F. Shi, Y.-C. Wang, T.-Z. Zhao, S. Zhang, T.-Y. Du, C.-B. Yang, Y.-H. Li and X.-Q. Sun, *PLoS One*, 2012, 7, e40365.
- 214 Y. Rolland, P. Marighetti, C. Malinverno, S. Confalonieri, C. Luise, N. Ducano, A. Palamidessi, S. Bisi, H. Kajiho, F. Troglio, O. G. Shcherbakova, A. R. Dunn, A. Oldani, L. Lanzetti, P. P. Di Fiore, A. Disanza and G. Scita, *Dev. Cell*, 2014, 30, 553–568.
- 215 S. B. Mamer and P. I. Imoukhuede, *Biomedical Engineering Society*, 2015, p. 001254.
- 216 G. Ascherl, C. Sgadari, R. Bugarini, J. Bogner, O. Schatz, B. Ensoli and M. Sturzl, AIDS Res. Hum. Retroviruses, 2001, 17, 1035–1039.
- 217 M. Hantera, H. Abd El-Hafiz and A. Y. Abdelnaby, *Egypt. J. Chest Dis. Tuberc.*, 2014, **63**, 751–754.
- 218 H. Takayama, Y. Miyake, K. Nouso, F. Ikeda, H. Shiraha, A. Takaki, H. Kobashi and K. Yamamoto, *J. Gastroenterol. Hepatol.*, 2011, **26**, 116–121.
- 219 P. W. Rosario, Arq. Bras. Endocrinol. Metabol., 2010, 54, 477–481.
- 220 Y. Lemos-Gonzalez, F. J. Rodriguez-Berrocal, O. J. Cordero, C. Gomez and M. Paez de la Cadena, *Br. J. Cancer*, 2007, 96, 1569–1578.
- 221 M. Nowak, B. Marek, J. Karpe, B. Kos-Kudla, L. Sieminska, D. Kajdaniuk and M. Treszer, Exp. Clin. Endocrinol. Diabetes, 2014, 122, 582–586.